Applied Catalysis B: Environmental 250 (2019) 250–272

Contents lists available at ScienceDirect

Applied Catalysis B: Environmental

journal homepage: www.elsevier.com/locate/apcatb

Review

Reforming of tar from biomass gasification in a hybrid catalysis-plasma system: A review

Lina Liu[a], Zhikun Zhang[a,b,**,1], Sonali Das[a], Sibudjing Kawi[a,*,1]

[a] Department of Chemical & Biomolecular Engineering, National University of Singapore, 117585, Singapore
[b] School of Energy and Environmental Engineering, Hebei University of Technology, Tianjin 300401, China

ARTICLE INFO

Keywords:
Biomass gasification
Tar
Catalytic reforming
Plasma reforming
Synergistic effect

ABSTRACT

The generation of tar in biomass gasification is highly undesirable since the condensation and agglomeration of tar causes clogging and contamination of downstream equipment, leading to low energy efficiency and high maintenance cost. Currently, the most widely used methods for tar reforming are catalytic reforming and plasma reforming. However, the main drawbacks for these two processes are: (i) the rapid catalyst deactivation caused by poisoning, sintering and coke deposition for catalytic reforming, and (ii) low energy efficiency, low selectivity of syngas and the formation of undesirable byproducts for plasma reforming. Recently, therefore, the hybrid plasma-catalysis system has attracted much attention for tar reforming, since it can overcome the above-mentioned drawbacks and generate a synergy effect. The addition of catalyst in plasma could change the discharge properties of plasma, and the plasma could also modify the catalyst property and change the status of reactants. At present, very few review articles have reported and compared the performances of tar reforming in the plasma-only, catalysis-only and hybrid plasma-catalysis system. Therefore, this review paper focus on: (i) the deactivation characteristics and modification methods of steam-reforming catalysts, as well as the mechanism of tar catalytic reforming; (ii) the performance of tar reforming in various plasma reactors and the reaction mechanism based on the analysis of byproducts and energetic plasma species; and (iii) the possible synergistic effect of plasma and heterogeneous catalyst in a hybrid plasma-catalysis system caused by the multiple interactions of plasma and catalysts.

1. Introduction

With the increasing interest in substituting fossil fuels and reducing greenhouse gas emissions, the utilization of biomass as renewable energy resources is of great importance for the world [1,2]. Currently, about 10% to 14% of the world's total energy consumption is provided by biomass [3,4]. Biomass can be utilized by various methods including pyrolysis [5–8], gasification [9,10], hydrothermal carbonization [11–13], and torrefaction [14–16], etc. Among them, gasification is one of the most promising methods to convert biomass to syngas via a series of thermochemical reactions at above 700 °C [17,18]. Syngas can be further used for producing synthesis fuels including Fischer-Tropsch fuels, methanol, dimethylether (DME), ethanol, etc., as well as for generating heat and electricity, as shown in Fig. 1 [19,20]. Besides, gasification of biomass can reduce emissions of CO_2, H_2S, SO_2, NO_x, etc. [21]. However, the presence of tar in syngas is a major challenge that limits the application of syngas and commercial development of biomass gasification [22].

Tar is defined as a complex mixture containing multiple condensable organic compounds such as monocyclic aromatic

Abbreviations: DME, dimethylether; PAHs, polycyclic aromatic hydrocarbons; WGSR, water-gas shift reaction; S/C, ratio of steam to carbon; EXAFS, X-ray absorption fine structure; DTG, differential thermogravimetry; TPO, temperature programed oxidation; SEM, scanning electron microscope; XRD, X-ray diffraction; HADDF, high-angle annular dark field; REOs, rare earth oxides; AAEM, alkaline earth metallic species; MNP, a-methylnaphthalene; WHSV, weight hourly space velocity; NPs, nanoparticles; RHC, rich husk char; LSNFO, $La_{0.8}Sr_{0.2}Ni_{0.8}Fe_{0.2}O_3$; NTP, non-thermal plasma; CD, corona discharge; PD, pulse discharge; DBD, dielectric barrier discharge; GAD, gliding arc discharge; MW, microwave; SEI, specific energy input; SPD, spark discharge; EOPR, externally oscillated gliding arc plasma reformer; LNAD, laval nozzle arc discharge plasma; OES, optical emission spectrograph; GC-MS, gas chromatography-mass spectrometer; FT-IR, Fourier transform infrared spectrometer; CatO, catalysis-only; PlO, plasma-only; PPC, post plasma-catalysis; IPC, in plasma-catalysis; DD, thermal decomposition

* Corresponding author.
** Corresponding author at: Department of Chemical & Biomolecular Engineering, National University of Singapore, 117585, Singapore.
E-mail addresses: zhangzk@hebut.edu.cn (Z. Zhang), chekawis@nus.edu.sg (S. Kawi).
[1] These authors contributed equally to the article.

https://doi.org/10.1016/j.apcatb.2019.03.039
Received 9 January 2019; Received in revised form 5 March 2019; Accepted 13 March 2019
Available online 15 March 2019
0926-3373/

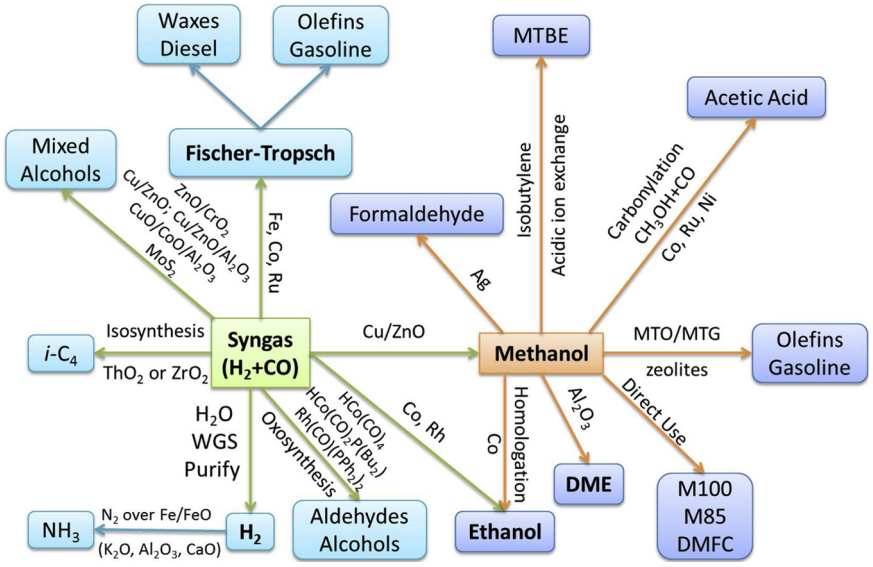

Fig. 1. Conversion technologies of syngas [19].

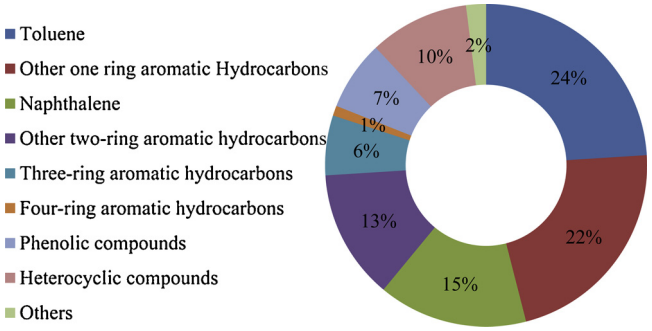

Fig. 2. Typical composition of biomass tar [3].

hydrocarbons, oxygen-containing hydrocarbons and complex polycyclic aromatic hydrocarbons (PAHs). It is also defined as an unspecific matter that include all organics existing in the synthetic gas apart from gaseous hydrocarbons (C1 to C6) and benzene [3]. The composition and concentration of tar differ significantly, depending on the reaction temperature, gasifier type and feedstock species, etc. The typical composition of tar from biomass gasification is shown in Fig. 2 [3]. The concentration of tar in raw syngas varies from 1 g/Nm^3 to more than 100 g/Nm^3 [23]. A much lower amount of tar is tolerable in downstream processing, ranging from about 1 mg/Nm^3 for chemical synthesis to 100 mg/Nm^3 for internal combustion engines [19,24]. Therefore, the removal of tar is essential for the development of biomass gasification [25,26].

The formation of tar in biomass gasification is undesirable, since it can be condensed and concentrated after the gasifier at lower temperature, leading to the clogging and contamination of downstream equipment. Meanwhile, tar formation reduces the energy efficiency of gasification process [27,28]. In recent years, many efforts have been made to remove the tar by physical/mechanic separation [29], thermal cracking [30], catalytic reforming [31,32], plasma reforming [33] and miscellaneous reforming [34,35], as presented in Fig. 3.

Tar can be physically separated from syngas using filter and oil/water wet scrubbing, but it causes secondary pollution. Meanwhile, the loss of chemical energy in tar results in a lower processing efficiency of biomass gasification [36]. The thermal cracking of tar need to be operated at high temperatures (> 1100 °C) to achieve efficient tar decomposition, and thus incurs higher energy consumption and maintenance cost [37,38]. Catalytic reforming is an efficient method for tar reforming, and various kinds of steam-reforming catalysts have been developed [36]. However, the rapid deactivation of catalysts caused by poisoning, sintering and coke deposition leads to the decline and even termination of tar reforming activity [28,39]. Plasma reforming is another promising technique for tar reforming, due to its fast ignition, high removal efficiency and universality for various hydrocarbons [33,40]. However, the plasma-induced chemical reactions are highly non-selective and the formation of unfavorable products cannot be avoided, which lead to lower selectivity of target products (such as syngas) [41]. Therefore, the integration of heterogeneous catalysts and plasma could be an attractive and promising alternative for conversion of tar into useful fuel gas, by overcoming the disadvantages of both catalytic reforming and plasma reforming [42,43]. For the hybrid plasma-catalysis system, the existence of plasma could change the physicochemical characteristics of catalysts and increase the catalytic activity and durability [44]. Meanwhile, the existence of catalysts in plasma reactor could limit the formation of undesirable byproducts and increase the selectivity of syngas [45].

Based on the above analysis, the reviewing of potential and efficient methods for tar reforming is of great importance, which is able to provide guidance for the future development of biomass gasification and tar removal. Previous review articles focused on summarizing different methods for tar reduction (including mechanical removal, partial oxidation, thermal cracking, catalytic reforming and plasma reforming) [46–48], and/or reviewing the development of different catalysts for steam reforming of tar (including Ni-based catalysts, other transition metal catalysts, alkali metal catalysts, natural mineral catalysts, zeolite catalysts and active carbon catalysts) [3,49,50]. However, the performance of tar reforming in catalysis-only (CatO), plasma-only (PlO) and hybrid plasma-catalysis processes, which are considered as potential methods for tar removal and have attracted increasing attention, has rarely been reviewed and reported previously. In this paper, therefore, the steam reforming of tar was reviewed from the following four aspects, including: (i) the deactivation mechanism and modification of steam-reforming catalysts, as well as the mechanism of tar reforming in a CatO system; (ii) the performance of different plasma reactors in tar reforming, the detection of byproducts and energetic radicals, and the mechanism of tar reforming in PlO system; (iii) tar reforming in different hybrid plasma-catalysis systems including pretreatment of steam-reforming catalysts by plasma, in plasma-catalysis (IPC) and post plasma-catalysis (PPC) systems, as well as the synergy and interactions between plasma and steam-reforming catalysts; and (iv) the future directions for tar reforming in a hybrid plasma-catalysis system.

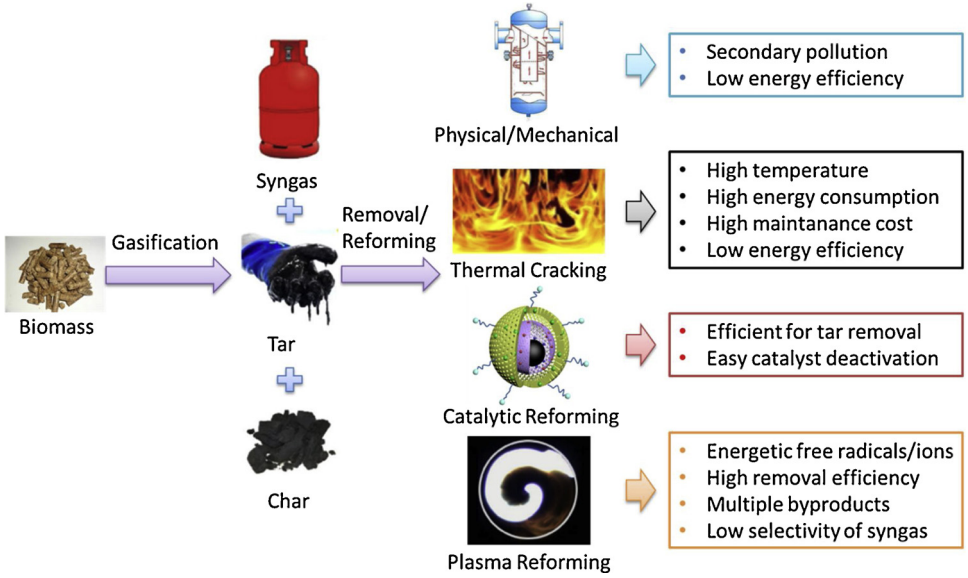

Fig. 3. Technologies for tar abatement and reforming.

2. Catalytic reforming of tar

Catalytic reforming has been considered as one of the most potential method for tar removal. However, the catalysts become deactivated easily by sintering, poisoning and coke, due to their high affinity to sulfur and chlorine, and low resistance to coke formation [51]. A variety of catalysts, including Ni-based catalysts [52,53], other transition metal catalysts [54,55], alkali catalysts [26,52], natural catalysts [32,56,57], zeolite catalysts [58] and active carbon (AC)/char-based catalysts [17,59,60], have been developed to increase the tar conversion, syngas selectivity, and resistance to coke formation [18,61,62].

2.1. Deactivation of tar reforming catalysts

Among different catalysts, Ni-based catalysts are recognized as the most promising in steam reforming of tar due to its high activity, low cost and easy regeneration [63]. Their superior catalytic activity should be attributed to the high reactivity of C—C and C—H bonds in tar compounds over Ni particles [35]. In addition, Ni can also activate the H_2O and CO_2, which participate in tar reforming and WGS reaction [28]. The major challenge that prevents the commercialization of catalytic reforming is the high cost caused by the deactivation and short lifetime of catalysts. The formation of carbon deposits and Ni particle growth in tar reforming are recognized as the most important factors that lead to the deactivation of catalysts [28,62,64]. The carbon deposited on surface of catalysts in tar reforming can be formed by the following reactions [65]:

$$CO \rightleftharpoons C(s) + CO_2 \quad (1)$$

$$CO + H_2 \rightleftharpoons C(s) + H_2O \quad (2)$$

$$C_nH_{2n} \rightleftharpoons nC(s) + nH_2 \quad (3)$$

Reaction (1) (Boudouard reaction) and reaction (2) are favorable at low temperatures, and reaction (3) is more important at higher temperatures. In addition, both reaction (1) and (3) are less important in the absence of catalysts.

The amounts, species and properties of carbon deposition vary significantly, depending on the reaction temperature, S/C (steam to carbon ratio), tar composition, and catalyst species [64,66,67]. According to previous studies, the carbon deposition can be divided into three types, i.e. C_I, C_{II}, and C_{III} based on the O_2-TPO analysis [68]. C_I represents a highly reactive carbonaceous species (amorphous external coke or encapsulating coke) on the surface of catalysts, corresponding to TPO peaks in the temperature range of 200 to 400 °C. C_I is easily accessible to react with steam to form CO and to oxygen during its combustion activated by catalysts. C_{II} species is generally observed at a higher temperature range of 300–500 °C. C_{II} represents polymerized carbonaceous species (graphitic and aromatic) with less reactivity with steam and a more condensate structure. It can be a precursor for the formation of carbon deposition with much lower reactivity. C_{III} is whisker carbon (filamentous coke) observed at the highest temperature of > 500 °C. It is not adsorbed on catalysts and almost has no reactivity with steam. This kind of carbon species shows no obvious contribution to the deactivation of catalysts since it grows towards the outside of catalyst particles. However, they increase pressure drop and may lead to dangerous bed blocking. Among three carbonaceous species, C_{II} plays an important role in the deactivation of catalysts by encapsulating the active metal sites [69].

Cao et al. [64] found that the content of carbon deposition decreased significantly with increasing the S/C molar ratio. The injection of stream in tar reforming reduced the formation of carbon deposition by promoting water-gas shift reaction (WGSR) (reaction 4), and thereby reducing the CO disproportionation as reaction (1) and (5) [70]. Kong et al. [67] tested the stability of different Ni-based catalysts for tar reforming. The results indicated that the deactivation of catalysts was caused by coke deposition, rather than the growth of Ni particles and the changes of catalyst structures.

$$H_2O + CO \rightleftharpoons H_2 + CO_2 \quad (4)$$

$$CO \rightleftharpoons C + O \quad (5)$$

Artetxe et al. [71] analyzed the carbon deposited on Ni/Al_2O_3 catalysts in steam reforming of different model tar compounds. The TPO results in Fig. 4 illuminated that filamentous carbon is more likely to be formed for reforming of furfural, and polymerized carbon for reforming of phenol and anisole. The SEM images (Fig. 5) confirmed that the furfural reforming resulted in a highly developed filamentous carbon deposited on the surface of catalysts. Non-structured carbon deposition was mainly formed for steam reforming of aromatic hydrocarbons.

Yung et al. [72] studied the deactivation mechanism of Al_2O_3-supported Ni-based catalysts for tar reforming using X-ray absorption fine structure (EXAFS) spectroscopy. They found that the oxidation of partial Ni to generate an oxide and/or a sulfide phase was likely to result in the deactivation of Ni-based catalysts with increasing time-on-stream and reaction cycles, rather than coke deposition, phosphorus poisoning,

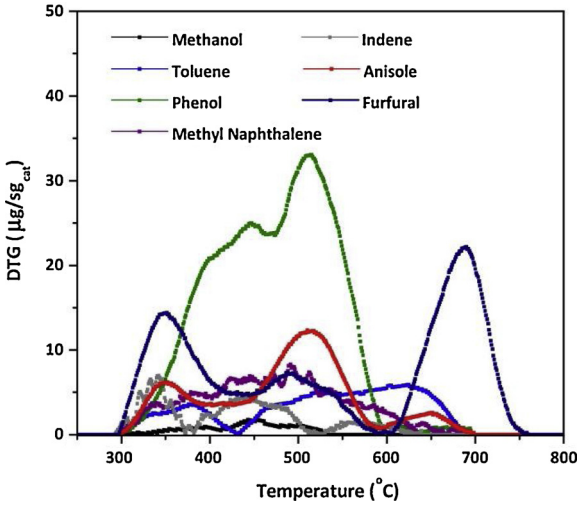

Fig. 4. DTG-TPO curves of the coke deposition on the catalyst for reforming of different model tar compounds [71].

or particle size changing. Specially, the sulfur poisoning and the contaminating compounds could not be removed completely in the regeneration process.

Based on the above analysis, it is essential to develop novel catalyst systems that can prevent the sulfur poisoning, the oxidation of Ni, and the formation of carbon deposition simultaneously.

2.2. Enhancement of catalytic performance

Active phase, promoter, support and synthesis method are the four most dominant factors influencing the performance of steam reforming catalysts [48,73]. Extensive studies have focused on the improvement of the catalytic performance by modifying active metals [68,74,75], adding a promoter [76–78], strengthening a support [79] or optimizing the preparation methods [73,80]. A summary of the modification methods of steam reforming catalysts is shown in Table 1.

2.2.1. Modification of active phase

The modification of active phase or metal, such as choosing metals with high activity or alloying with secondary metals, leads to a higher catalytic activity, better resistance to coke deposition and sulfur poisoning [68,74,75]. Ni-based catalysts have been extensively applied for tar reforming due to the low cost and high activity of Ni particles [63,81]. Al_2O_3 is generally used as the supports in many cases [82]. However, the main problem of Ni/Al_2O_3 catalyst for tar reforming is the rapid deactivation caused by encapsulation of carbon, and sintering or agglomeration of active Ni particles at high temperatures and high pressures [81].

Fe in different oxidation states is also potentially effective for destruction of C—C and C—H bonds in aromatic hydrocarbons such as benzene, toluene etc. [83]. The lower cost of Fe than Ni provides higher potential economic possibility in biomass gasification industries [84]. The application of a Fe/olivine catalyst in toluene reforming obtained a three times higher toluene conversion of 91% and hydrogen yield of 0.066 mol H_2/h/g-cat than that with olivine [83]. Characterization results indicated that the high percentage of Fe^0 contributed to the breaking of C—C and C—H bonds in toluene. The presence of a small quantity of Fe_3O_4 promoted the WGSR [85].

Noble metals, such as Pt, Ru, Pd, Ir, and etc., exhibited higher activity and better resistance to coke formation and sulfur poisoning in tar reforming [86]. Almost all tar can be converted to syngas in the presence of noble metal catalysts [48]. The amount of coke deposition was much smaller than that with Ni catalysts, due to the higher combustion activity of noble metals [87]. However, they were not frequently used due to the high cost [61,88]. In most cases, trace amounts of noble metals were used as promoter of Ni-based catalysts [61,89,90].

The use of bimetallic catalysts such as Ni-Fe, Ni-Co, Fe-Zn, Ni-Cu catalysts, is also a promising alternative to increase the catalyst activity [56,68,75]. Among these, Ni-Fe has been proven to be effective in tar reforming [74]. Zou et al. [91] found that the Fe_3Ni_8/Palygorskite catalyst showed higher catalytic activity and stability than the monometallic catalysts of Fe_3/Palygorskite and Ni_8/Palygorskite and Palygorskite, as shown in Fig. 6(a). The superior catalytic performance of Fe_3Ni_8/Palygorskite catalyst was attributed to the formation of highly dispersed Fe-Ni alloy on Palygorskite. Fe and Ni elements showed the same distribution patterns in HADDF image (Fig. 6b), which were highly dispersed on the surface of Palygorskite. The result confirmed the strong interaction between Fe and Ni in Fe_3Ni_8/Palygorskite catalyst.

Based on the above analysis, the formation of alloy for the bimetallic catalysts is potential for the modification of active metals by a cost-saving method, which contributes to a higher catalytic activity and stability by generating a synergy.

2.2.2. Addition of promoters

The addition of promoter is able to increase the activity and stability of catalysts and promote the gasification of carbon [76–78]. The effects of promoters on catalytic performance mainly include increasing oxygen vacancies and oxygen mobility, changing the basicity, enhanced the interaction of metal and support and improving the dispersion of active metals. The rare earth oxides (REOs) [92], alkali metals [93] and alkaline-earth metals [94,95] are all regarded as effective promoter of

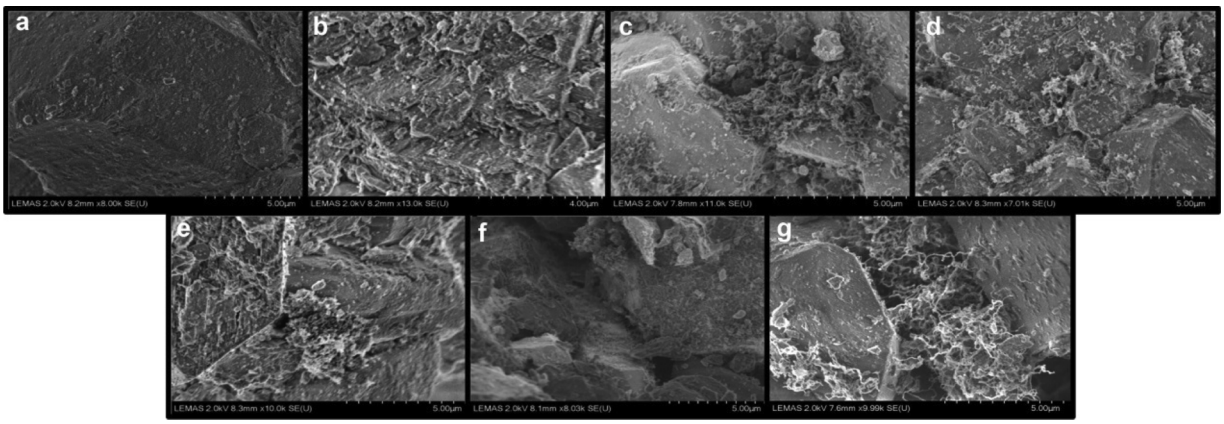

Fig. 5. SEM imagines of the (a) fresh and used catalyst for steam reforming of (b) toluene, (c) phenol, (d) methyl naphthalene, (e) indene, (f) anisole and (g) furfural [71].

Table 1
Modification of steam reforming catalysts.

Modification method	Active metal	promoter	support	Preparation method	Tar compounds	Condition	X_{tar} (%)	Comments	Ref.
Modification of active metals	Ni		Al_2O_3	Impregnation	Phenol	T = 650˜800 °C, S/C = 13, reaction time = 40 min	8˜57	Both the carbon conversion efficiency and H_2 potential obtained the maximum of 81% and 59% at 750 °C with a low coke amount of < 5 wt.%.	[128]
	Fe		Olivine	Impregnation	Toluene	T = 825 °C, S/C = 2	91	Fe (10 wt.%) supported on olivine calcined at 1000 °C contributed to a toluene conversion of 91% and H_2 production of 0.066 mol H_2/h/g-cat, which was three times higher than that with olivine.	[83]
	Ni-Fe		Palygorskite	Co-precipitation	Toluene	T = 700 °C, S/C = 1, reaction time = 48 h	> 97	Bimetallic Fe_3Ni_8/Palygorskite exhibited higher catalytic performance than the monometallic Fe_3/Palygorskite and Ni_8/Palygorskite. Its superior catalytic performance should be caused by the highly dispersive Fe-Ni alloy on Palygorskite.	[91]
Addition of promoters	Ni	CeO_2 and MgO	Olivine	Impregnation	Toluene	T = 790 °C, S/C = 5	89	The catalytic activity followed an order of Ni-Ce-Mg/olivine > Ni-Ce/olivine > Ni/olivine. The addition of Ce and Mg enhanced the catalytic performance of Ni/olivine catalyst by reducing the activation energy of coke combustion and promoting coke gasification.	[98]
	Ni	K, Ca, and Mn	Dolomite	co-impregnation	Toluene	T = 800 °C, S/C = 3	42˜62.2	The effect of promoters on the catalytic activity followed an order of Ni–Mn/dolomite > Ni–Ca/dolomite > Ni–K/dolomite > Ni/dolomite.	[81]
Enhancement of supports	Ni		MCM-41	Impregnation	Real tar from gasification of wood sawdust	T = 800 °C		The application of Ni/MCM-41 in gasification of wood sawdust promoted the formation of H_2, and valueable bio-oil byproducts, and reduced the formation of coke. The superior performance of Ni/MCM-41 should be attributed to the highly dispersed NiO particles, abundant specific surface area, and pore volume.	[111]
	Ni		Char	One-step pyrolysis	Actual tar from pyrolysis of RH	T = 500˜900 °C	92.3˜100	RH char supported Ni catalyst was effective for tar reforming, with a highest toluene conversion of 100% and lowest liquid byproduct yield of 10.7% at 900 °C. In addition, the catalyst exhibited outstanding stability which can be used effectively for 5 cycles.	[115]
	Ni		CaO–Al_2O_3	Co-precipitation	Toluene	T = 650 °C, S/C = 1	70	The Ni–Ca–Al catalyst (8:62:30) with an optimum composition showed better catalytic performance compared with other Ni-Ca-Al catalysts, which should be attributed to the enhanced basic strength and high resistance to agglomeration at high temperatures.	[107]
Optimization of preparation methods	Ni-Fe		olivine	Wet impregnation and thermal fusion	Phenol	T = 850 °C, S/C = 1	˜100	Partial Fe was fused into the structure of olivine and (Mg, Fe)Fe_2O_4 was formed as a new phase for TF-Ni/Fe/olivine. TF-Ni/Fe/olivine exhibited higher activity than WI-Ni/Fe/olivine, due to the strengthened interaction between active metal and support.	[56]
	Ni		MCM-41	Ethylene glycol (EG) assisted impregnation	Real tar from gasification of sunflower stalk	T = 550-750 °C		Ni/MCM-41-EG catalyst exhibited a better dispersion of NiO with smaller particle size and a stronger interaction of active metal and support, compared with Ni/MCM-41. All these properties contributed to the higher catalytic performance of Ni/MCM-41-EG.	[109]
	Ni		MgO	Impregnation, co-precipitation and hydrothermal	Methanol	T = 700 °C, S/C = 3	97.4	The highest methanol conversion of 97.4%, and hydrogen yield of 58.5% was achieved over the nano Ni_xMg_yO-hydro prepared by a hydrothermal method. The “isolation effect” of the Ni_xMg_yO solid solution structure and the high basicity of Ni_xMg_yO-hydro surface were proven to contribute to the excellent catalytic performance of Ni_xMg_yO-hydro.	[125]

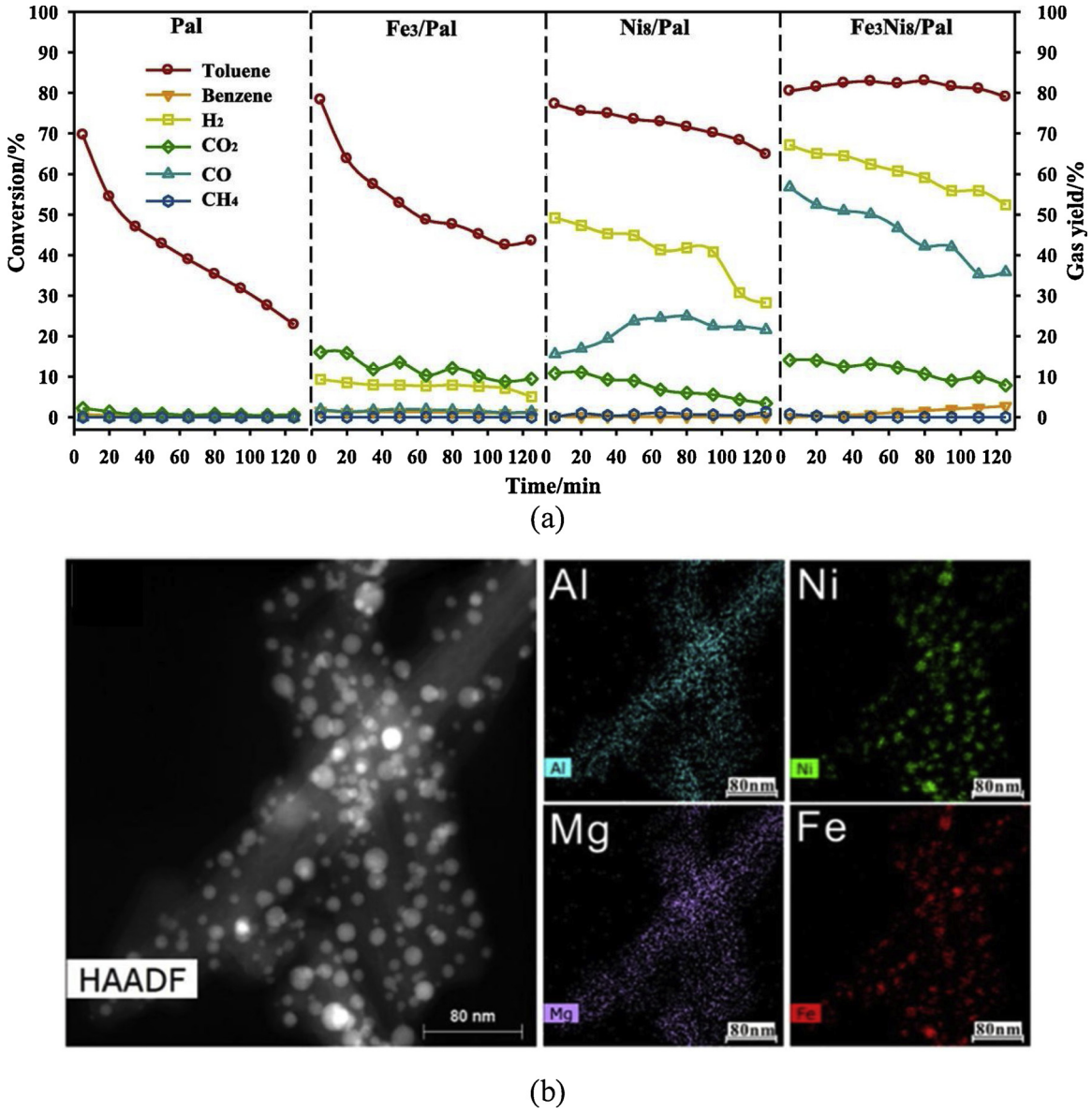

Fig. 6. (a) Catalytic performance of Pal, Fe_3/Pal, Ni_8/Pal and Fe3Ni8/Pal catalysts for toluene reforming, and (b) HADDF image of Fe_3Ni_8/Pal catalyst and the elements distributions [91].

steam reforming catalysts.

REOs, as redox promoters, are able to improve the oxygen storage capacity and metal-support interaction of catalyst [77,96]. CeO_2 is recognized as a more promising REOs compared with La and Pr, due to its superior oxygen transfer capability and oxygen storage capacity [97,98]. The addition of Ce (1 wt.%) in Ni (3 wt.%)/olivine resulted in an increase of toluene conversion from 59% to 88%. In addition, the Ce modified Ni/olivine exhibited high resistance to coke deposition and H_2S poisoning [98]. Kawi et al. [92,99,100] demonstrated that the addition of CeO_2 improved the dispersion of Ni and the reducibility of NiO particles, and enhanced the interaction of Ni and CeO_2, leading to an outstanding catalytic performance of the CeO_2 doped Ni-based catalysts.

The alkali and alkaline earth metallic species (AAEM), such as Na, K, Ca, and Mg can also be used as promoters for steam reforming catalysts, since AAEM can promote the transmission of OH and H radicals from catalyst to tar, especially for K [94,101,102]. Ashok et al. [69] demonstrated that the CaO doped Ni-Fe/Fe_2O_3-Al_2O_3 with a Ca:Fe:Al molar ratios of 1.5:1:2 achieved the best catalytic performance with a toluene conversion of more than 80% for a period of 22 h [69]. Kim et al. [103] studied the effect of K, Ca and Sr on the catalytic performance of Ni/γ-Al_2O_3 for steam reforming of glycerol. The results revealed that the addition of AAEM slightly decreased the glycerol conversion. Meanwhile, the coke formation was reduced, leading to a higher long-term stability. The Sr promoted catalysts exhibited outstanding resistance to coke deposition and long-term stability for more than 100 h, which was attributed to the increased basicity of catalyst, and promoted adsorption of steam and the decreased adsorption of coke.

2.2.3. Enhancement of supports

The supporting materials play important roles in catalyst performance by (i) interacting with active phases; (ii) increasing the mechanical strength and thermal stability; (iii) providing surface for dispersion of active phases; (iv) playing a chemical role in catalysis, and (v) changing the distribution of products [18,82]. Various support materials can be used, including acid supports (γ-Al_2O_3) [71,104,105], basic supports (MgO and CaO) [106,107], REOs (CeO_2 and La_2O_3), zeolites (SBA-15, ZSM-5 and MCM-41) [108–111], natural and synthetic minerals (olivine, dolomites, hydrotalcite, perovskite and

palygorskite) [112–114] and biochar [115–117]. A support with higher surface area, higher mechanical strength and thermal stability is more promising in improving the dispersion of active metals, suppressing the aggregation of metals and controlling the particle size efficiently [79].

Zeolites are regarded as promising supporting materials due to their porous structure and high BET surface area [118]. The uniform and highly dispersed Ni-Fe alloy supported on SBA-15 led to a strong interaction of active phase and support, contributing to a high biomass conversion to gaseous products of ˜90% at 600 °C [119]. Wang et al. [120] demonstrated that the superior catalytic performance of Ni/SBA-15 should be attributed to (i) outstanding anti-coke ability caused by the highly-dispersed small Ni particles and well-ordered diffusion routes of reactants, intermediates and products; (ii) higher interaction between metal and support; (iii) better resistance to sintering caused by the spatial restriction of support [109].

Natural minerals, including olivine and dolomites, were extensively applied as the supports for steam reforming catalysts because of their low cost, nontoxicity and disposability [57]. However, the natural mineral supported catalysts show less potential due to their low activity on the reforming of PAHs [121]. As a consequence, synthetic minerals, such as spinel, perovskite, hydrotalcite and palygorskite, were preferred to use because of the formation of small metal NPs (nanoparticles), high dispersion of active metals and strengthened interaction of active metal and support [80]. Ashok et al. [107] demonstrated that the hydrotalcite-derived Ni–Ca–Al (8:62:30) catalyst with an optimum catalyst composition exhibited a toluene conversion of 70% stably for 24 h. The characterization of catalysts indicated that the lower agglomeration of Ni particles, higher basicity of catalyst, and lower rate of coke formation (2.5 $mgC{\cdot}g^{-1}\,h^{-1}$) contributed to the high activity and stability of Ni–Ca–Al (8:62:30).

Char supported catalysts show potential for the *in situ* reforming of tar derived from biomass gasification, which simplifies the subsequent tar removal processes [17,59,115,122]. In the study of Guo et al. [60], the application of rich husk char (RHC)-supported catalysts in tar cracking not only reduced tar formation significantly, but also changed the product distribution of tar compounds, as shown in Fig. 7. The transformation of larger PAHs to light tar compounds such as phenol and 4-methyl-phenol was promoted over RHC-supported catalysts, especially for RHC-Fe. Shen et al. [17,59,115] studied the *in situ* conversion of tar over RHC-supported Ni-Fe catalysts, which exhibited much more advantages of convenient synthesis and energy-saving. The RHC played significant roles in tar removal in two aspects: (i) it acted as an intermediate reductant for the reduction of metal oxides and CO_2; and (ii) it served as an adsorbent for the adsorption of metal ions and tar.

2.2.4. Improvement of preparation methods

The preparation methods also significantly affect the physicochemical properties, morphology and particle size of catalysts [73,80,123,124]. Luo et al. [125] compared the catalytic performance of Ni_xMg_yO prepared by impregnation (Ni_xMg_yO-impre), co-precipitation (Ni_xMg_yO-copre) and hydrothermal (Ni_xMg_yO-hydro) for steam reforming of methanol. Ni_xMg_yO-hydro showed the highest methanol conversion of 97.4% and hydrogen production of 58.5%, and no detectable coke deposition. The characterization of catalysts indicated that the isolation effect of Ni_xMg_yO solid solution structure contributed to the superior resistance to coke deposition, by reducing the aggregation of Ni nano particles. Meng et al. [56] found that the structure and morphology of TF-Ni/Fe/olivine prepared by thermal fusion was significantly changed compared with calcined olivine (Fig. 8), and a new (Mg, Fe)Fe_2O_4 phase was formed by mingling partial Fe into the structure of olivine. The TF-Ni/Fe/olivine exhibited a smaller particle size of Ni-Fe alloy than WI-Ni/Fe/olivine prepared by wetness impregnation, because of the reorganization of active metal and olivine support during thermal fusion. TF-Ni/Fe/olivine exhibited better catalytic performance compared with WI-Ni/Fe/olivine in terms of conversion of phenol and naphthalene, long-term stability. It should be attributed to the enhanced interaction of Ni-Fe alloy and olivine support for TF-Ni/Fe/olivine, which provided more stable active sites.

Catalysts prepared by hydrothermal, thermal fusion and co-precipitation show more potential in increasing the catalytic activity and stability than that synthesized by traditional wetness impregnation. However, impregnation is still widely applied for catalyst synthesis due to the easies preparation procedure and low cost. As a consequence, appropriate synthesis methods should be chosen according to different application of catalysts [18].

2.3. Catalytic mechanism

Tar is decomposed and converted into small molecular gaseous products via a series of thermochemical reactions including thermal cracking, dry and steam reforming, as Reaction (6)–(9) [121,126].

$$\text{Thermal cracking: } pC_nH_x\ (\text{tar}) \rightarrow qC_mH_y\ (\text{smaller tar}) + rH_2 \quad (6)$$

$$\text{Dry reforming: } C_nH_x\ (\text{tar}) + nCO_2 \rightarrow (x/2)H_2 + 2nCO \quad (7)$$

$$\text{Steam reforming: } C_nH_x\ (\text{tar}) + nH_2O \rightarrow (n + x/2)H_2 + nCO \quad (8)$$

$$\text{Carbon formation: } C_nH_x\ (\text{tar}) \rightarrow nC + (x/2)H_2 \quad (9)$$

Jess [127] investigated the mechanism and kinetics of thermal cracking of aromatic hydrocarbons (naphthalene, toluene and benzene) in the range of 700 °C to 1400 °C. Fig. 9 showed that benzene was the most dominant product for thermal cracking of aromatic hydrocarbons. The carbonaceous residue (soot) was mainly produced by the cracking of naphthalene. The formation pathway of coke deposition in catalytic reforming of naphthalene could be divided in two steps, which has been summarized in Fig. 10. Naphthalene underwent dehydrogenation in the first step, and the residual hydrogen of hydrocarbon fragments was further dehydrogenated and the adsorbate layer was transformed to graphic carbon.

Artetxe et al. [128] demonstrated that the mechanism for steam reforming of phenol over Ni/Al_2O_3 catalysts could be explained in two possible pathways, which were both initiated with the dissociation of O—H followed by (i) the cracking of benzene ring caused by the cleavage of C—H and C=C bonds in position 2 and 6; (ii) the dissociation of C=O bonds and the subsequent rupture of C—H and C=C bonds. Both decomposition pathways led to the formation of H_2, CO and light hydrocarbons.

Oemar et al. [129] proposed the mechanism of steam reforming of toluene over $La_{0.8}Sr_{0.2}Ni_{0.8}Fe_{0.2}O_3$ (LSNFO) based on the catalyst characterization, as reaction (10)-(25). Firstly, water was adsorbed on the support and dissociated to produce H_2 and oxygen species. Secondly, toluene was decomposed to form methyl species and benzene on the metal site of LSNFO, where benzene was further cracked to acetaldehyde (C_2 species). Thirdly, aldehyde species was formed by the reaction between the oxygen species and C_2 species or methyl species. Fourthly, aldehyde species was decomposed to CO and H_2, or reacted further with oxygen species to form CO_2. Finally, the adsorbed CO, CO_2, and H_2 were desorbed into the gas phase.

Step 1: Dissociation of H_2O on support site (s2).

$$H_2O + s2 \rightleftharpoons O{\cdot}s2 + H_2 \quad (10)$$

Step 2: Decomposition of toluene on metal site (s1) to form C2 species.

$$C_7H_8 + s1 \rightleftharpoons C_7H_8{\cdot}s1 \quad (11)$$

$$C_7H_8{\cdot}s1 + s1 \rightleftharpoons C_6H_6{\cdot}s1 + CH_2{\cdot}s1 \quad (12)$$

$$C_6H_6{\cdot}s1 + 2s1 \rightleftharpoons 3C_2H_2{\cdot}s1 \quad (13)$$

Step 3: Reaction between C2 species and oxygen species.

$$C_2H_2{\cdot}s1 + O{\cdot}s2 \rightleftharpoons C_2H_2O{\cdot}s1 + s2 \quad (14)$$

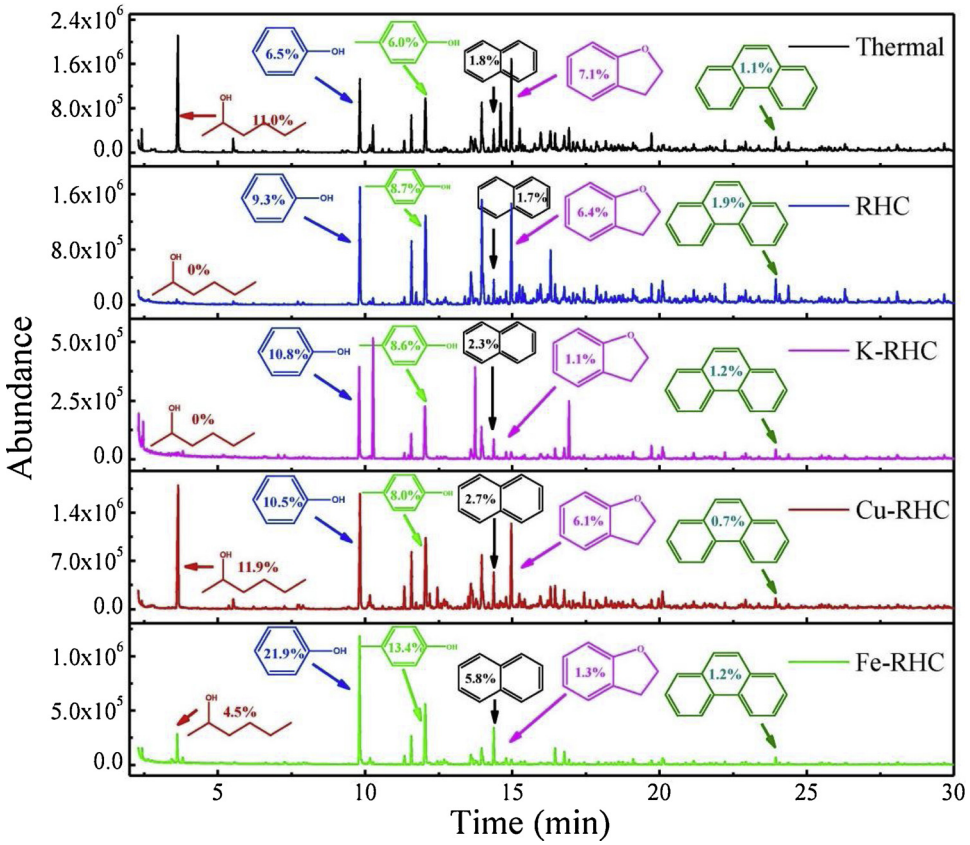

Fig. 7. GC–MS spectra of tar compounds over different RHC-supported catalysts [60].

$$C_2H_2O{\cdot}s1 + s1 \rightleftharpoons CH_2O{\cdot}s1 + C{\cdot}s1 \quad (15)$$

$$CH_2{\cdot}s1 + O{\cdot}s2 \rightleftharpoons CH_2O{\cdot}s1 + s2 \quad (16)$$

$$CH_2O{\cdot}s1 + s1 \rightleftharpoons CHO{\cdot}s1 + H{\cdot}s1 \quad (17)$$

Step 4: Formation of CO and CO_2.

$$CHO{\cdot}s1 + s1 \rightleftharpoons CO{\cdot}s1 + H{\cdot}s1 \quad (18)$$

$$CO{\cdot}s1 + O{\cdot}s2 \rightleftharpoons CO_2{\cdot}s2 + s1 \quad (19)$$

$$CHO{\cdot}s1 + O{\cdot}s2 \rightleftharpoons CO_2{\cdot}s2 + H{\cdot}s1 \quad (20)$$

$$C{\cdot}s1 + CO_2{\cdot}s2 \rightleftharpoons 2CO + s1 + s2 \quad (21)$$

Step 5: Desorption of products.

$$CO{\cdot}s1 \rightleftharpoons CO + s1 \quad (22)$$

$$CO_2{\cdot}s2 \rightleftharpoons CO_2 + s2 \quad (23)$$

$$2H{\cdot}s1 \rightleftharpoons H_2{\cdot}s1 + s1 \quad (24)$$

$$H_2{\cdot}s1 \rightleftharpoons H_2 + s1 \quad (25)$$

Shen et al. [17] summarized the mechanism for *in situ* conversion of tar over Ni-Fe catalysts supported on char derived from pyrolysis of rice husk, as presented in Fig. 11. Biomass was initially decomposed to permanent gases, liquid tar and solid char via pyrolysis reactions. Tar could be reformed to produce H_2 and CO in the presence of RHC-supported Ni-Fe catalysts. Then partial RHC-supported catalysts were transformed to SiO_2-based catalysts since it contained high amount of amorphous SiO_2 (nano size) in RH char. Finally, the Fe and Ni in RHC-supported catalysts could be recovered by the thermal regeneration of catalysts due to the high sublimation temperatures of Ni and Fe (2732.0 °C and 1535 °C, respectively). In general, RH char played important roles in biomass pyrolysis by acting an intermediate reductant for the reduction of metal oxides and CO_2, as well as serving as an adsorption support for the adsorption of metal ions and tar.

3. Plasma reforming of tar

Even though the catalytic reforming technology has been

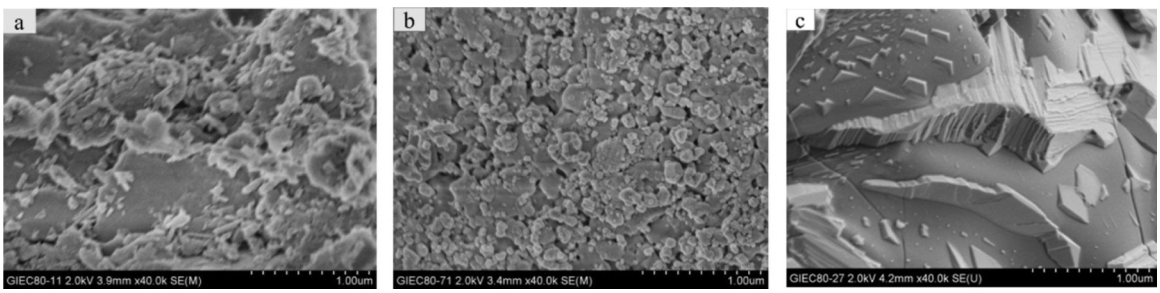

Fig. 8. SEM images of (a) raw ore, (b) WI-Ni/Fe/olivine, and (c) TF-Ni/Fe/olivine [56].

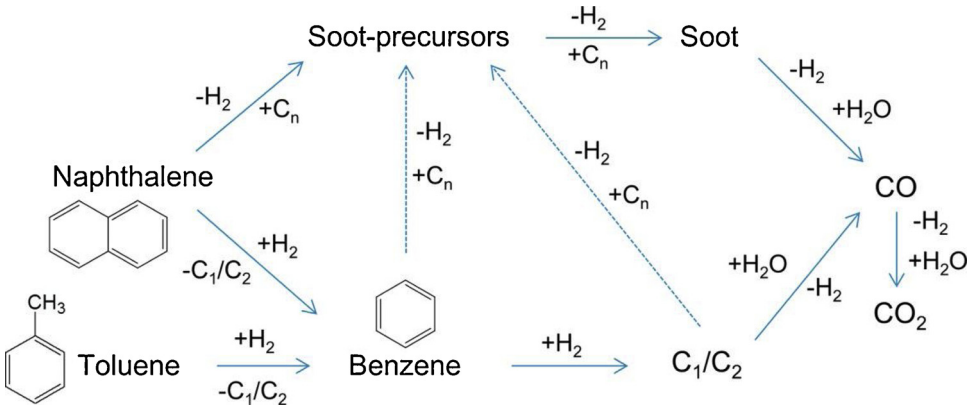

Fig. 9. Pathway for thermal cracking of naphthalene, toluene and benzene in the presence of H_2 and steam [28,127].

extensively studied, the easy deactivation of catalysts still remains the main challenge. Therefore, the application of plasma in tar reforming can be a promising alternative approach due to the high tar conversion efficiency, universality for various compounds, the presence of highly excited particles and compact design [33,40,130]. Compared with thermal and catalytic processes, the overall energy consumption of plasma process can be reduced significantly due to higher reaction rate and fast achievement of steady state, providing a promising alternative for clean fuel production [131].

3.1. Design of plasma reactor

Plasma can be divided into thermal plasma and non-thermal plasma (NTP) (non-equilibrium plasma), depending on the temperature, energy level and electronic density [132]. For thermal plasma, the gases can reach a temperature of higher than 1700 °C, and all energetic and neutral species are in thermal equilibrium [133]. For NTP, the overall temperature of gases can remain at room temperature, while the energetic electrons with high temperature of 10^4 °C to 10^5 °C and high energy level of 1 eV–10 eV can be produced at normal gas temperatures [33]. Therefore, most chemical bonds in hydrocarbons can be easily cleaved, which overcomes the drawbacks of high temperature required for thermal and catalytic reforming and enables the occurrence of thermodynamically unfavorable chemical reactions at ambient conditions [131]. The typical NTP reactor for removal and reforming of tar contains corona discharge (CD), pulse discharge (PD), dielectric barrier discharge (DBD), gliding arc discharge (GAD) and microwave (MW) plasma [134]. A performance comparison of tar destruction in different plasma reactors has been summarized in Table 2. The high energy consumption and low tar conversion are the main disadvantages of CD plasmas [135]. Even though thermal, GAD and MW plasmas are all proven to be efficient with high tar removal efficiency, the formation of abundant coke deposition limit their development [35]. The application of DBD plasma in tar reforming seems to be more attractive since it is much easier to be integrated with heterogeneous catalysts as a hybrid plasma-catalysis system, due to the lower yield of coke [136]. Consequently, DBD plasma was most frequently used in the hybrid plasma-catalysis system in previous studies [137].

3.1.1. Thermal plasma

Thermal plasma can be used for tar removal. The gas products from biomass pyrolysis/gasification, containing abundant condensable organics and particles, can be converted into a tar-free hydrogen-rich syngas [147,148]. Simultaneously, inorganic particles and ashes are converted into inert, environment-stable and vitreous materials [149]. Fourcault et al. [150] developed a kinetic model containing fifteen reactions to evaluate the removal of toluene and naphthalene using a plasma torch. The results showed that the conversion efficiency of both tar model compounds reached high values of > 99.9% for toluene (with an energy efficiency of > 23.2 g/kWh) and 96.7% for naphthalene (with an energy efficiency of 22.4 mg/kWh). Eliott et al. [146] studied the destruction of tar in a microwave plasma torch. Tar was destroyed completely and the main products of tar reforming were recognized as CO, H_2, CO and solid carbon. However, the high specific energy consumption of 796 kJ/gtar under optimized operation conditions was a great challenge for tar reforming. In addition, the erosion and

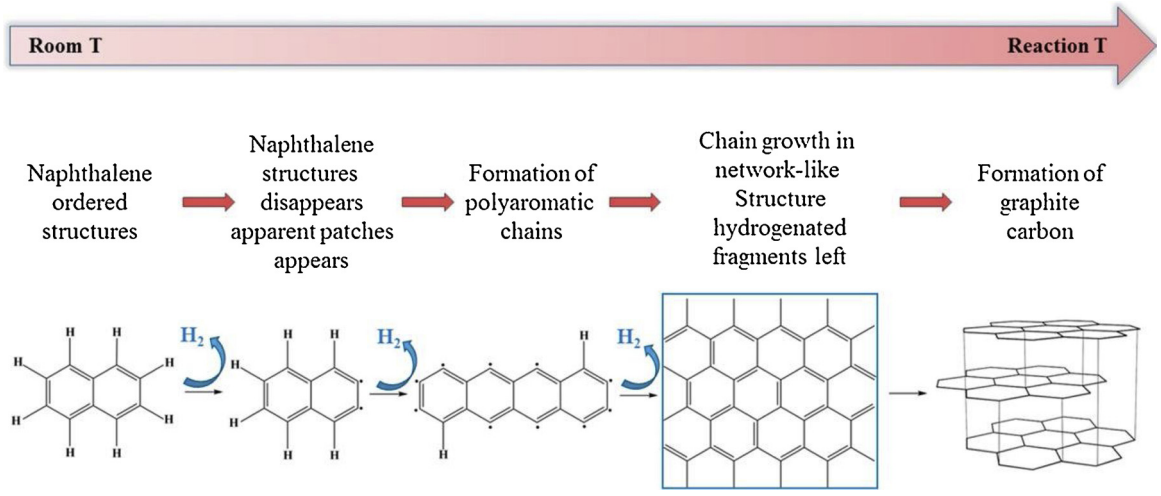

Fig. 10. Pathway for the formation of graphite carbon from catalytic reforming naphthalene [56].

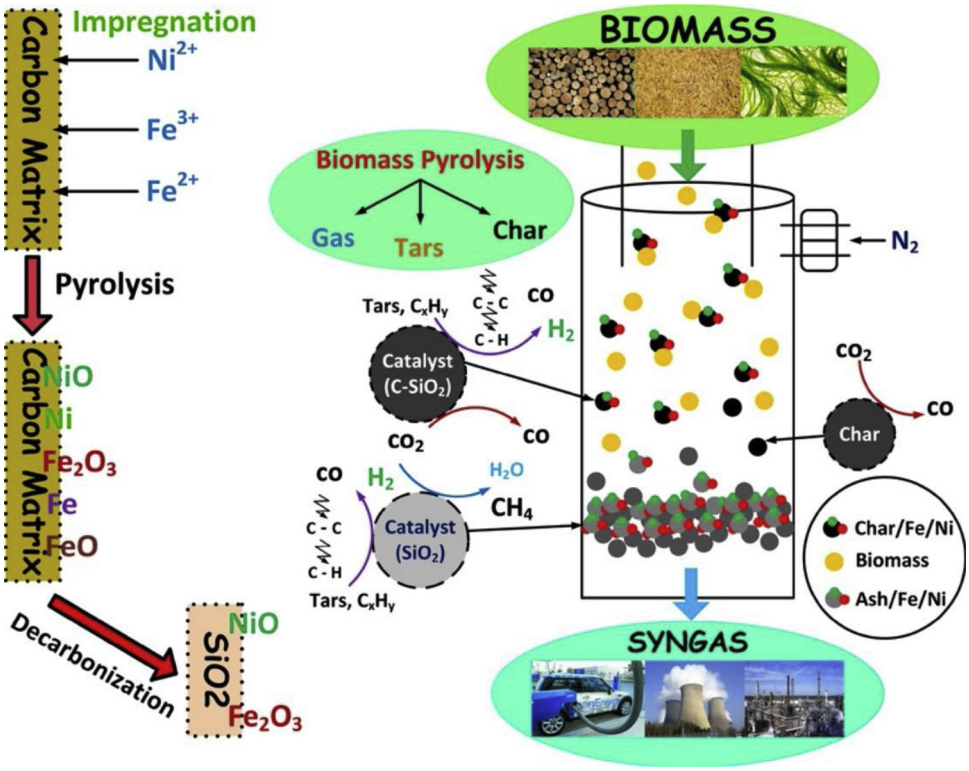

Fig. 11. Mechanism of *in-situ* tar conversion over RH char-supported Ni–Fe catalysts in biomass pyrolysis [17].

Table 2
Performance comparison of tar reforming in plasma reactors.

Plasma	Tar	Carrier gas	Tar content (g/Nm^3)	Q[a] (m^3/h)	SEI[b] kWh/m^3	X[c] %	EE[d] g/kWh	Ref
CD	C_7H_8	$He+H_2O$	261	0.005	3.6	35	25.3	[133]
CD	C_7H_8	Dry air	70	0.015	0.58	50	2.5	[138]
AC GAD	C_7H_8	N_2+H_2O	23.5	0.23	0.19	42	27	[33]
AC GAD	C_7H_8	N_2	10	0.24	1.9	95	5.92	[139]
AC GAD	C_6H_6	N_2+H_2O	4.3	1	0.17	83	20.9	[140]
DC GAD	$C_{10}H_8$	O_2	1.3	0.4	0.47	92	3.6	[141]
3-electrode GAD	$C_{10}H_8$	N_2+H_2O	14.3	1.1	1	79	47	[142]
DBD	C_7H_8	Dry air	261	0.006	6.0	78	34	[143]
DBD	$C_{10}H_8$	$N_2+H_2+CO+CO_2$	90	0.3	0.06	60	2.2	[144]
DBD	C_7H_8	H_2	20	0.0024	4.1	99	4.79	[145]
Microwave torch	C_7H_8	20%Ar + N_2	4.2	1.07	0.93	99	4.5	[146]
MW	C_7H_8	N_2+H_2O	10	1.2	1.67	98	5.8	[40]

[a] The total gas flowrate.
[b] Specific energy input, SEI(kWh/m^3) = Discharge power(kW)/total gas flow rate(m^3/h).
[c] The conversion efficiency of tar compounds (%).
[d] Energy efficiency, EE(g/kWh) = Converted tar(g/m^3)/SEI(kWh/m^3).

evaporation of the electrodes caused by the extremely high temperature are also the major drawbacks of thermal plasma [151].

3.1.2. Corona discharge plasma

CD plasma is regarded as one of the most promising approaches for tar removal and reforming. The optimal temperature for tar reforming is about 400 °C [19]. Nair et al. [135,152] investigated the reforming of naphthalene, toluene and phenol as model tar compounds in a pulse corona discharge plasma reactor. The results indicated that the tar conversion increased with increasing CO_2 concentration in the feed gas, due to the formation of O radicals. However, the tar conversion was negatively affected by the presence of CO because of the consumption of O particles by CO. In addition, the operation cost for tar removal in CD plasma accounted for 20% of the total electrical output from biomass gasification, leading to high energy consumption and the infeasibility of large scale application [135].

3.1.3. Dielectric barrier discharge plasma

Reforming of tar to syngas and light hydrocarbons in DBD plasma reactor has attracted increasing attention [153–155]. In DBD plasma, the excited electrons transferred their energy to the reactants by collision, leading to the cleavage of C—C and C—H bonds in tar compounds with dissociation energies of 3 eV to 4 eV. The excited radicals generated from collision can recombine to gases and light hydrocarbons [156,157].

Saleem et al. [130,145] applied the DBD plasma for the treatment of syngas (a mixture of H_2, CO and CO_2) containing toluene as tar model compound. The results showed that the toluene conversion efficiency increased with rising the discharge power and residence time. In addition, the increase of temperature led to the reduction of solid residue (completely disappeared at 400 °C) and the increase of selectivity and yield of lower hydrocarbons. Nevertheless, the toluene conversion and CO yield decreased due to the combination of CO and O radicals at

higher temperatures [155]. Similar results were also reported by Liu et al. [143]. In Taghvaei et al.'s study [158], the application of DBD plasma could remove anisole as the representative product of lignin pyrolysis efficiently. Helium was recognized as a potential carrier gas, which would lead to higher anisole conversion due to the more stable and homogeneous discharge than that observed with argon and hydrogen [159]. Moreover, the residence time of reactants and excited species was proven to be an important parameter for anisole conversion and product distribution, and the most prevalent species was recognized as the phenoxy derived from the cleavage of C_{methyl}-O bond.

Tar reforming using DBD plasma gained increasing attention due to its simplicity, scalability, and the availability of reliable, efficient and affordable power supplies [160]. However, the low power density and energy efficiency caused by low current and gas temperature limited its application.

3.1.4. Gliding arc discharge plasma

The advantages of compact design, high conversion efficiency, easy control on reactions, fast starting and responding characteristics and low energy consumption for GAD plasma make it promising for tar reforming [140,142,161]. GAD plasma is generally regarded as a transitional plasma type. Most of the gliding arc power (up to 75–80%) is dissipated in the non-equilibrium zone with a dissipated power of 40 kW/electrode pair [139]. GAD plasma reactor can be used flexibly in a wide variety of flowrate and discharge power (even to several kV) efficiently. Closely to a thermal plasma, GAD plasma exhibited much higher electron density of 10^{23}~10^{24} m^{-3} than other NTP, such as CD and DBD plasma [162]. All the above features contribute to the great potential for tar removal.

The oxidation steam reforming of syngas containing toluene and naphthalene was investigated in a GAD plasma [163]. The conversion of naphthalene and toluene reached more than 90% for reforming tar with energy efficiency of 62.5 g/kWh for naphthalene and 215 g/kWh for toluene at low tar content of 30 g/m^3. For tar with a high content of 75 g/m^3, the conversion efficiency of naphthalene and toluene decreased to 70% with energy efficiencies of 93.6 g/kWh and 369 g/kWh for naphthalene and toluene, respectively. Zhu et al. [139] developed a novel rotating GAD reactor for toluene reforming, which produced a stable and wide three-dimensional discharge zone. The dynamic behavior of a single discharge is shown in Fig. 12(a). The breakdown of a single discharge cycle of GAD occurred at t_0 when the gap between the electrodes was the narrowest, and the voltage dropped abruptly (Fig. 12b). Then the arc was prolonged with increasing time from t_1 to t_3, followed by the quenching and a new breakdown of arc at t_4. Simultaneously, the voltage increased with time and reached a maximum of 3120 V at t_4, and then a new discharge cycle started. They found that the novel rotating GAD was more promising in toluene reforming, with a highest toluene conversion of 95.16%, and energy efficiency of 16.61 g/kWh, which were much higher than that of MW and GAD plasma [164]. However, the high carbon deposition remained a great challenge for the application of the rotating GAD plasma in toluene reforming.

3.1.5. Microwave plasma

Microwave (MW) plasma is another effective method for converting light hydrocarbons [165] and CO_2 [166] into valuable fuel products of CO and H_2. The potential of MW plasma in tar reforming should be attributed to: (i) the electrodeless property that can overcome electrode erosion caused by the oxidizer (such as oxygen and steam) and high temperature [167]; (ii) the accessibility of an advanced and complicated power source; and (iii) the vibrational excitation distribution of energy [168].

Jamróz et al. [40] developed a MW plasma reactor for the reforming of model tar surrogates including toluene, benzene and 1-methylnaphthalene. The increase of tar feed concentration and gas flowrate resulted in the reduction of tar conversion efficiency, while the addition of steam promoted the tar conversion and reduced the formation of undesirable byproducts obviously. They also found that the presence of CO_2 and H_2 in the feed gas promoted the conversion of tar due to the generation of O, OH and H radicals in plasma core zone [23]. Sun et al. [134] found that the reforming of toluene in the MW-metal discharge cracking produced significant amounts of soot, which was considered as the main challenge for the application of MW plasma in tar reforming.

3.1.6. Other types of plasma

In addition to the above plasma reactors, other NTP, such as spark discharge (SPD) plasma [169], externally oscillated gliding arc plasma reformer (EOPR) [170], and Laval nozzle arc discharge (LNAD) plasma [151], are also used for tar reforming. Ethanol was reformed to syngas of C_2H_2, C_2H_4, CH_4, CO_2, CO and H_2 by a LNAD plasma reactor, with a maximum ethanol conversion of 90% at an optimum S/C of 2 and O/C of 1.6 [151]. A benzene conversion efficiency of 90.7% and an energy efficiency of 22.95 g/kWh were achieved with optimized parameters for the EOPR plasma [170]. The features of higher discharge density and channel temperature, higher conversion of reactants and lower energy consumption make the SPD plasma a promising alternative for tar reforming, compared with other NTP [169,171].

3.2. Detection of byproducts and energetic particles

A series of reactions between excited molecular, atoms, ions, free radicals occurred in plasma reactor, leading to the formation of abundant byproducts [35]. Thus, the detection and analysis of intermediate energetic particles and the end byproducts contributes to the demonstration of the complex reaction mechanism in plasma.

Liu et al. [33] analyzed the energetic radicals by optical emission

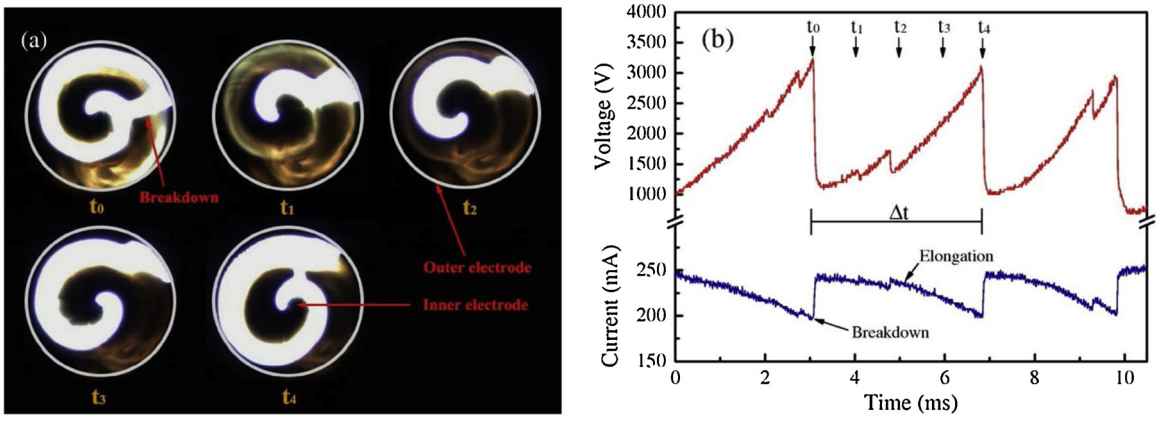

Fig. 12. (a) Dynamic behavior and (b) the voltage and current waveforms of the rotating GAD plasma [139].

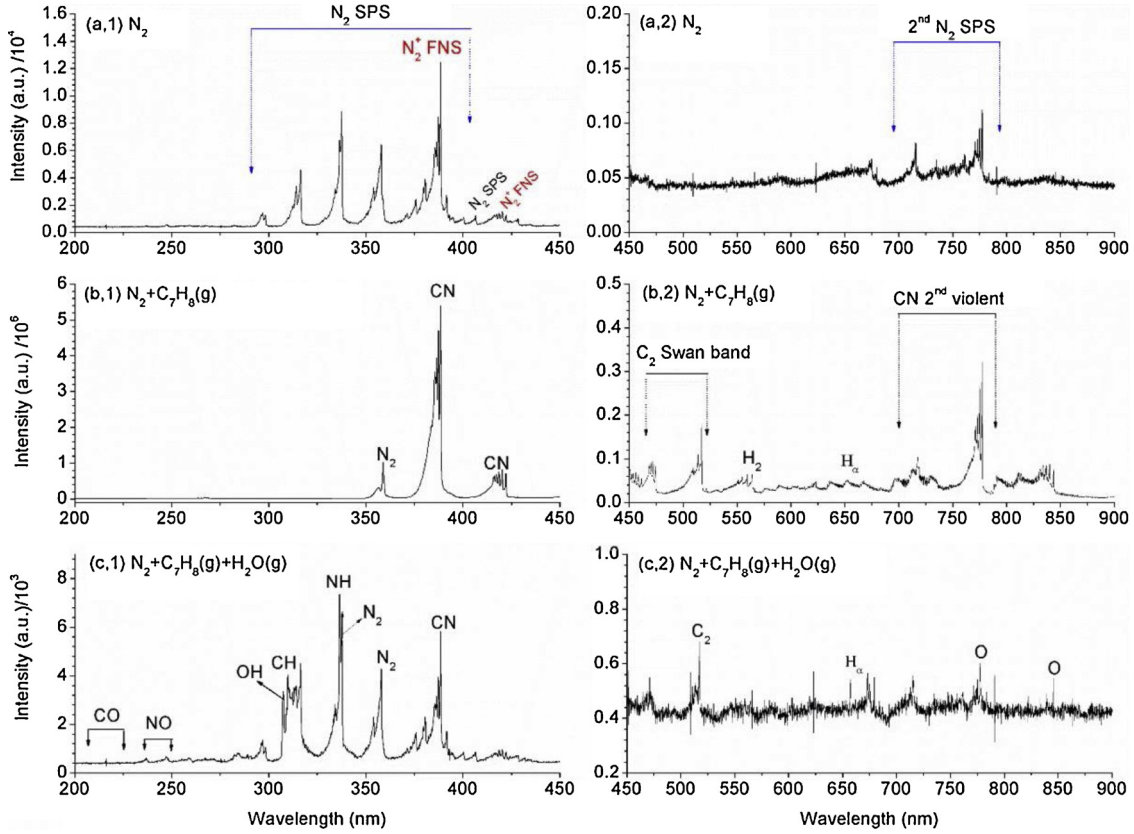

Fig. 13. Optical emission spectra of GAD plasma in the atmosphere of (a) N_2; (b) N_2/C_7H_8; and (c) $N_2/C_7H_8/H_2O$ [33].

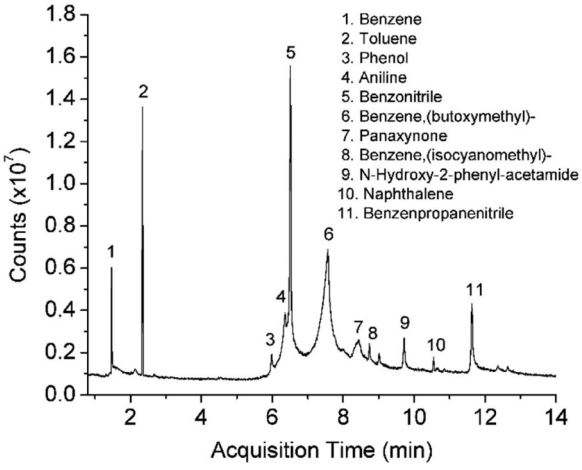

Fig. 14. GC–MS spectra of byproducts in steam reforming of toluene in GAD plasma reactor [33].

spectrograph (OES) and the end byproducts using gas chromatography-mass spectrometer (GC–MS) in steam reforming of toluene in GAD plasma, as shown in Figs. 13 and 14. Strong CN ($B^2\Sigma \rightarrow X^2\Sigma$) violet and second order violet band were detected, together with the hydrogen Nalmer series Hα (653.3 nm) and C_2 swan bands (460 nm to 520 nm) in reforming of N_2/C_7H_8 without steam, where the CN might be produced via reactions (26) to (29). The addition of steam in N_2/C_7H_8 reforming led to the generation of OH ($A^2\Sigma \rightarrow X^2\Pi$) from reactions (30) and (31). In addition, a NH ($A^2\Sigma \rightarrow X^2\Sigma$) band was also observed at 336.1 nm, which might be generated by the reactions of N atoms and H_2O or OH radicals (reactions 32–33), since NH was not detected in N_2/C_7H_8 without steam [172]. The presence of CO ($A^1\Pi \rightarrow X^1\Pi$) at 200 nm to 220 nm, CH ($C^2\Pi^+ \rightarrow X^2\Pi$) at 314.3 nm and NO ($A^2\Sigma^+ \rightarrow X^2\Pi$) bands at 230 nm to 250 nm were also observed, where NO might be produced via reactions (34) and (35). Eliott et al. [146] found that free radicals of H_α, H_β, and O^+ were detected in the optical emission spectra of H_2O cracking. The presence of these radicals prevented the cracking of toluene to form larger molecules.

$$N_2 + C_2 \rightarrow CN + CN \quad (26)$$

$$N + CH_2 \rightarrow CN + H_2 \quad (27)$$

$$N + CH \rightarrow CN + H \quad (28)$$

$$N_2 + C \rightarrow CN + N \quad (29)$$

$$H_2O + e \rightarrow H + OH + e \quad (30)$$

$$H_2O + N_2^* \rightarrow H + OH + N_2 \quad (31)$$

$$N + H_2O \rightarrow NH + OH \quad (32)$$

$$N + OH \rightarrow NH + O \quad (33)$$

$$N + OH \rightarrow NO + H \quad (34)$$

$$NH + O \rightarrow NO + H \quad (35)$$

The species and amounts of liquid byproducts differs significantly depending on the tar compounds, species of plasma reactor, and operation parameters [33,77,139,143,173,174]. Fig. 14 shows that benzonitrile, benzene and benzenpropanenitrile were the dominant liquid byproducts. The N-containing compounds might be produced from the combination of NH_x or CN with intermediates of toluene cracking; naphthalene from the combination of cyclopentadienyl, and panaxynone from the cracking of a toluene ring and the subsequent recombination of the resulting fragments [33]. Zhu et al. [139] demonstrated that the dominant liquid byproducts contained phenylethyne, benzonitrile, indene and naphthalene for toluene reforming in a rotating GAD plasma, where the polymerization reactions were more

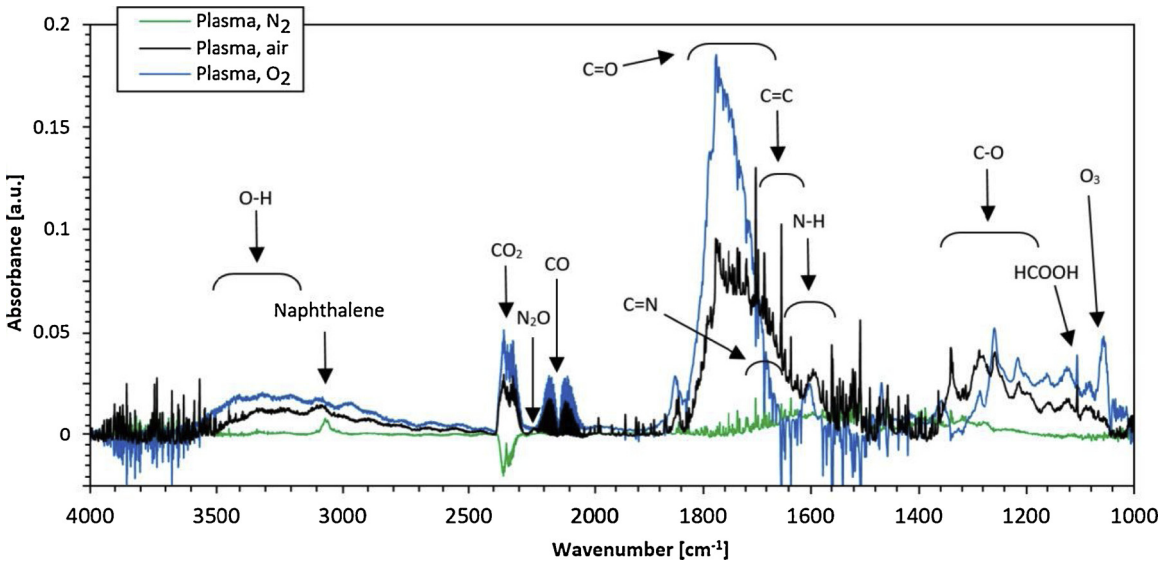

Fig. 15. FT-IR spectra of gas and solid byproducts derived from naphthalene reforming using DBD plasma with different carrier gases [160].

active.

Fourier transform infrared spectrometer (FT-IR) has been used for the analysis of end byproducts of tar reforming in plasma reactor [144,175]. Cimerman et al. [160] analyzed the gaseous and solid byproducts from naphthalene reforming in DBD plasma using FT-IR, as presented in Fig. 15. The main gas products contained CO, CO_2, N_2O, O_3 and HCOOH. The absorption bands of the organic functional groups (C═O, C═C, C═N, N−H and O−H) were also observed, indicating the formation of various hydrocarbons in naphthalene reforming. 1,4-naphthoquinone and phthalic anhydride were identified as the byproducts by the detailed analysis.

3.3. Reaction mechanism

Reaction mechanism of tar reforming in plasma reactors are complex due to the formation of multiple ions, free radicals and excited molecules [35]. The reaction mechanism was deduced based on the detection of energetic particles and end byproducts, as well as the most thermodynamically favorable reactions [143].

Decomposition of tar compounds could be initiated by energetic electrodes, ions and free radicals in plasma. Taking toluene as an example, toluene can be decomposed as reactions (36) to (45) [176]. The produced radicals could recombine to form different end byproducts such as CH_4, C_2H_6, C_2H_4, and C_3H_8, etc. The presence of steam also resulted in the formation of oxidized products such as CO and CO_2, etc. [33].

$$C_6H_5CH_3 + e \rightarrow C_6H_5 + CH_3 + e \quad (36)$$

$$C_6H_5CH_3 + e \rightarrow C_6H_4 + CH_3 + H + e \quad (37)$$

$$C_6H_5CH_3 + e \rightarrow C_5H_5 + C_2H_2 + e \quad (38)$$

$$C_6H_5CH_3 + e \rightarrow C_3H_3 + C_4H_4 + e \quad (39)$$

$$C_6H_5CH_3 + O^+/{O_2}^+/N^+/{N_2}^+ \rightarrow C_6H_4 + {CH_3}^+ + O/O_3/N/N_2 \quad (40)$$

$$C_6H_5{CH_3}^+ + e \rightarrow C_6H_5 + CH_3 \quad (41)$$

$$C_6H_5CH_3 + N_2 (A^3\Sigma_u^+) \rightarrow C_6H_5 + CH_3 + N_2 \quad (42)$$

$$C_6H_5CH_3 + N_2 (a^1\Sigma_u^-) \rightarrow C_5H_6 + C_2H_2 + N_2 \quad (43)$$

$$C_6H_5CH_3 + N_2 (A^3\Sigma_u^+) \rightarrow C_6H_5CH_2 + H + N_2 \quad (44)$$

$$C_6H_5CH_3 + N_2 (A^3\Sigma_u^+) \rightarrow C_6H_4CH_3 + H + N_2 \quad (45)$$

The reaction pathway of toluene reforming in GAD plasma was proposed by Liu et al., as shown in Fig. 16 [33]. Toluene was initially decomposed by the H-abstraction in the methyl group by excited N_2 or energetic electrons [177], since C–H bond in methyl group possesses the smallest dissociation energy of 3.7 eV, compared with the C−H bond in benzene ring (4.3 eV), C−C bond between methyl and benzene ring (4.4 eV), C−C bond benzene ring (5.0 eV–5.3 eV) and C═C bond in benzene ring (5.5 eV) [178]. The produced benzyl radicals could combine with OH to form benzaldehyde. Benzene, phenol, aniline and benzonitrile were formed by the combination of H, OH, NH_2 and CN radicals and phenyl radicals [175]. Besides, the combination of benzyl and methyl radicals led to the formation of ethylbenzene, which further reacted with CN to generate benzene (isocyanomethyl). Another way for toluene reforming might be the oxidation of benzene ring to form a stable epoxide [179], which could be attacked by energetic species, generating CO and H_2 eventually.

Sun et al. [134] summarized the reaction mechanism of toluene reforming in MW plasma, as presented in Fig. 17. Four reaction routes were proposed, which were initiated by the H-abstraction and CH_3 abstraction in the presence of energetic electrodes and excited N_2 species, via reactions (42)–(45). The produced C_6H_5 was converted to *ortho*-benzyne (*o*-C_6H_4), which could be further cracked to C_2H_2 and C_4H_2 via route (2). Indene could be generated by the combination of benzyl radical and acetylene followed by ring closure via route (1). The abstraction of C_2H_2 in phenyl radical followed by the addition of methyl and H radical resulted in the formation of 3-methylhexane (route 4). The combination of aromatic radicals led to the formation of more complicated structures such as PAHs and soot via route 1 and 3.

Based on the above analysis, the single plasma system exhibited high removal efficiency of tar even at room temperature. However, multiple byproducts were produced in the presence of abundant energetic electrons, ions and free radicals, leading to a low energy efficiency and complicated reaction mechanism. In addition, the low selectivity of syngas caused by the uncontrollable formation of products in plasma remains a great challenge for the commercial application of plasma in tar reforming.

4. Tar reforming in a catalysis-plasma reactor

A synergistic effect of plasma and heterogeneous catalysts might be achieved in a hybrid plasma-catalysis system, aiming to overcome both disadvantages of lower product selectivity for plasma reforming and easy catalyst deactivation for thermal catalytic reforming [180]. NTP is generally applied in a hybrid plasma-catalysis system, since thermal

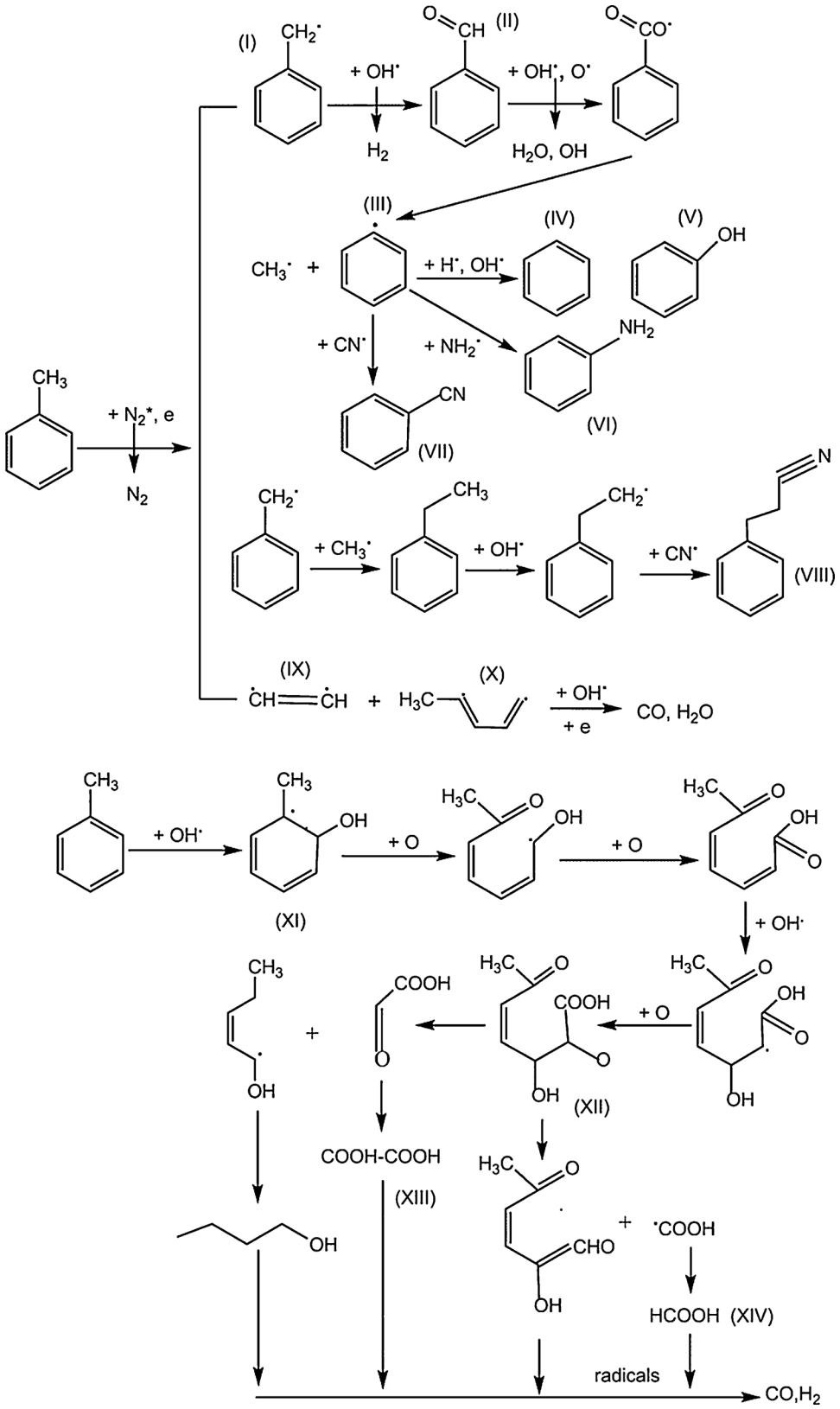

Fig. 16. Possible reaction mechanism for toluene reforming [33].

plasma is not able to be combined with catalysts because of high gas temperature [180].

4.1. Combination of catalysts and plasma

As shown in Fig. 18(a)-(c), plasma and catalysts can be combined by different methods, such as the pretreatment of catalysts using NTP, installing the catalysts downstream of NTP (i.e. post plasma-catalysis,

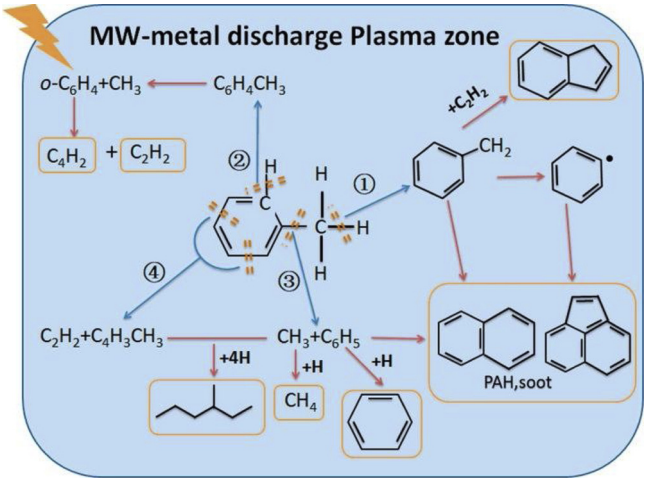

Fig. 17. Possible reaction pathway for toluene reforming in MW plasma [134].

PPC) and locating the catalysts in the discharge zone of NTP (i.e. in plasma-catalysis, IPC). For both PPC and IPC system, heterogeneous catalysts can be installed in the reactor as coating on the electrode or reactor wall, as a packed bed (granules, coated fibers, pellets), or as a layer of power, pellet, granules and coated fiber, as presented in Fig. 18(d) [181]. A performance comparison of CatO, PlO, PPC and IPC systems for the reforming of toluene as model tar compound is shown in Table 3, in order to demonstrate the synergistic effect of combining NTP and heterogeneous catalysts. It can be seen that tar could be decomposed efficiently only at high temperatures of over 600 °C for CatO system [74,182]. Plasma reforming of tar could be initiated even at room temperature, leading to lower overall energy cost and lower risk of catalyst deactivation [33,139]. However, the low selectivity of syngas and the formation of multiple undesirable byproducts remains the main limitation. The integration of catalysts in the PPC system was proven to promote the tar conversion as well as the syngas formation, compared with CatO and PlO systems [133]. However, the mechanism of tar reforming in PPC did not show obvious difference with that in PR system, since the short lifetime reactive plasma species were not able to interact with catalysts in downstream of discharge zone [35]. Differently from the PPC system, tar reforming in the IPC system not only increased the tar conversion and syngas selectivity, and the mechanism was also significantly changed due to the interaction of short lifetime reactive plasma species and catalysts, leading to much less species of liquid byproducts [35].

In view of economic point, catalytic reforming of tar is considered as a promising alternative, since a high purity of syngas can be obtained and simultaneously the fuel value is increased [3]. However, the deactivation of catalysts caused by coke deposition, sulphur and chlorine poisoning and sintering remains the most important challenge. As a consequence, some catalysts including nickel, cobalt and platinum catalyst for steam reforming of tar are still in laboratory stage due to the economic reason [183]. Plasma reforming is potential in overcoming the limitation of cost and deterioration of the catalysts [33]. In addition, plasma reforming is generally operated at low temperature and only a few hundred watts of power are required for the direct excitation of electrons [184]. The advantages of compactness, low weight, and mineral cost of simple metallic or carbon electrodes and simple power supply also contribute to the higher economic efficiency of PlO system compared with traditional CatO [185]. The main disadvantages of plasma reforming are the lack of selectivity towards desired process and inefficient utilization of the excited radicals, which result in high energy consumption [35]. A combination of plasma and catalyst as a hybrid plasma-catalysis system is able to reduce the cost of tar reforming compared with PR and CatO processes. It should be ascribed to the synergistic effect of plasma and catalysts that (1) the catalyst surface is activated at lower temperature and the catalyst deactivation caused by coke deposition, sintering and poisoning is reduced in plasma compared with CatO process; and (2) the undesired reactions are suppressed in the presence of catalysts compared with PlO process [186]. Therefore, the hybrid plasma-catalysis system is more promising than CatO and PlO systems from an economic and technical point of view.

4.1.1. *Pretreatment of catalysts by plasma*

Plasma technology, typically NTP, has been extensively used in the preparation and pretreatment of catalyst, due to its simple and rapid preparation procedure, easy control, low energy consumption and low cost [187]. Catalyst pretreatment by plasma results in better catalytic performance than pretreatment by conventional thermal reduction/oxidation and ultrasound methods [188]. The catalysts can be activated by plasma through removing capping ligands that used during the preparation of catalysts without sintering [189], changing the chemical status of catalyst surface at room temperature [190], and building defects or introducing atoms that are able to improve catalytic activity [191,192]. The application of plasma in catalyst preparation can reduce the particle size of catalysts, increase the metal dispersion, promote the reduction of active metals, increase the oxygen vacancy, and change the pore structure of catalysts [44,188]. Catalysts pretreated by plasma have been widely used in waste gas treatment [193,194], Fisher-Tropsch synthesis [195–197], reforming of methane to syngas [180,187], DeNO$_x$ [198,199] and tar reforming and syngas purification [200].

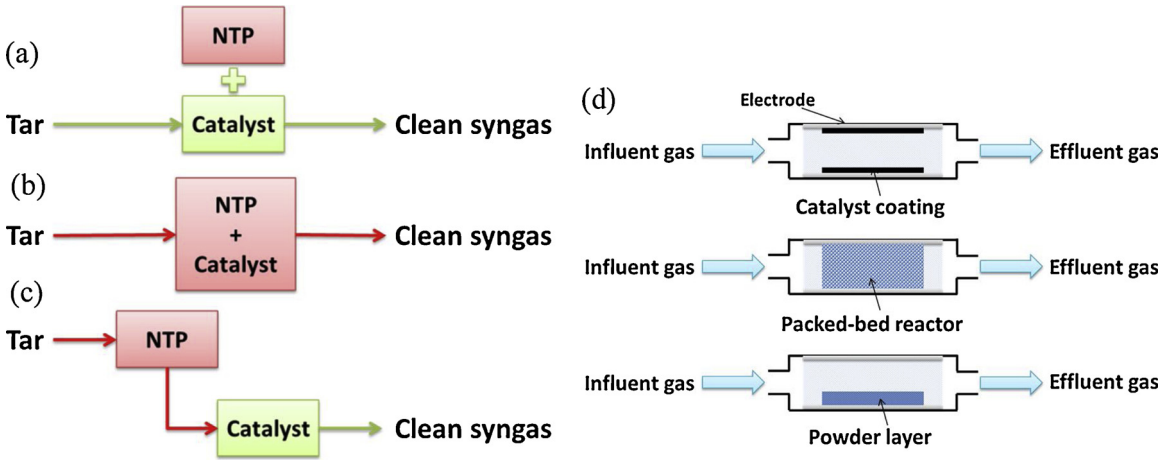

Fig. 18. Schematic overview of three hybrid plasma-catalysis system, (a) pretreatment of catalysts by plasma, (b) PPC, and (c) IPC system, and (d) the most commonly used catalyst insertion methods in IPC system [181].

Table 3
Performance comparison of toluene reforming as model tar compounds in CatO, PlO, PPC and IPC systems.

Method	Plasma type	T (°C)	Tar content (g/m^3)	Catalyst	S/C	X[a] (%)	S(H_2) (%)	S(CO) (%)	EE[b] (g/kWh)	Ref.
CatO	N.A.	650	77	Ni(10 wt%)/Fe_2O_3-Al_2O_3	3.4	80.9	32.5	49	N.A.	[74]
	N.A.	650	77	$LaNi_{0.8}Fe_{0.2}O_3$	3.4	67.1	26.9	47.7	N.A.	[182]
	N.A.	500	260	Ni(5 wt%)/SiO_2	1	32.8	7.0	13.1	N.A.	[133]
PlO	GAD	RT	23.5	No catalyst	2	35.8	23	25	46.3	[33]
	RGAD	RT	10	No catalyst	0	96	36	0	6	[139]
	DC	500	260	No catalyst	1	34	2.7	4.7	24.5	[133]
PPC	DC	500	260	Ni(5 wt%)/SiO_2	1	57	11.9	17.2	41	[133]
	DBD	300	173	Ni(5 wt%)/ZSM-5	1	79.5	43	13	20.7	[35]
IPC	DBD	160	17.7	Ni(10 wt%)/Al_2O_3	2.5	42	29	0	2	[42]
	DBD	300	173	Ni(5 wt%)/ZSM-5	1	86.5	63.3	18.2	22.5	[35]
	DBD	300	173	Ni1Al3	1	96	57	11	25	[137]

[a] The conversion efficiency of toluene (%).
[b] Energy efficiency, EE = converted tar (g/h)/Discharge power (kW).

Wang et al. [187] found that the glow discharge plasma treated NiMgSBA-15 exhibited higher catalytic activity and stability compared with the untreated one, due to the reduced size of Ni clusters and strengthened metal-support interaction [201]. The formation of filamentous and encapsulating carbon was inhibited effectively over the plasma treated catalyst, while large amount of graphitic carbon was produced on the surface of untreated catalyst, leading to the catalyst deactivation [202]. Moreover, the stronger basic sites by plasma treatment promoted the chemisorption of CO_2 and enhanced the coke elimination. The confinement effect of the pore channels in the mesoporous SBA-15 efficiently prevented the sintering of metallic Ni particles. Similar results were observed by Yu et al. [203]. Plasma treatment was able to enhance the dispersion of Ni particles, while the reduction degree of Ni/MgAlO catalyst was reduced. The addition of Pt facilitated the reduction of nickel, and consequently the plasma-treated Ni–Pt catalyst obtained high catalytic activity and promoted suppression of coke formation.

Besides, plasma could also be used for the regeneration of coked catalysts, with the advantage of shorter treatment time and higher efficiency without internal catalyst disturbances [204]. HafezKhiabani et al. [200] demonstrated that both pin-to-plate DBD plasma and low-pressure RF plasma could remove the coke on the Pt–Sn/Al_2O_3 catalyst efficiently, with decoking yields of ˜100% for DBD plasma and 59% for RF plasma, respectively. The specific surface area, pore volume, metal distribution and the Pt–Sn interaction of the regenerated catalysts did not show obvious difference compared with the fresh samples, indicating that the plasma treatment method had no influence on the internal structure of catalysts.

Based on the above analysis, the advantages of pretreatment and regeneration of catalysts using plasma technique provide a promising alternative for the synthesis of steam-reforming catalysts with high catalytic activity, stability, and coke resistance, and easy regeneration.

4.1.2. Tar reforming in post-plasma-catalysis

The interaction between NTP and heterogeneous catalyst seems to be simple since the short lifetime reactive plasma species produced by plasma are not able to reach the catalysts in the downstream of the discharge zone in a PPC process [35]. Therefore, the plasma in PPC system mainly changes the feed composition in the catalyst reactor. For example, CH_4 can be converted to C_2 species (C_2H_2 and C_2H_4) in the discharge zone of plasma, which can be converted easily in the thermal catalytic process at a lower temperature than CH_4 [180].

Du et al. [205] found that the addition of Ni/γ-Al_2O_3 in the downstream of a non-thermal arc plasma reactor resulted in an increase of ethanol conversion and H_2 production, as well as a reduction of energy consumption for H_2 production from 68.5 to 40.1 kJ/mol. Tao et al. [133] compared the performance of toluene reforming in direct thermal decomposition (DD), CatO, PlO and PPC systems. An order of DD < CatO < PlO < PPC for toluene conversion efficiency were observed. The synergistic effect of NTP and Ni/SiO_2 catalyst could be explained in two aspects. On one hand, energetic electrons, ions and radicals were generated in the presence of plasma, leading to the acceleration of toluene conversion and the increase of catalyst activity. On the other hand, the existence of Ni/SiO_2 favored the formation of CO and H_2, leading to a higher toluene conversion and syngas selectivity. In addition, the stability of Ni/SiO_2 catalyst was improved in the presence of plasma by enhancing its resistance to coke formation.

4.1.3. Tar reforming in in-plasma-catalysis

Tar reforming in the IPC process can achieve higher tar conversion efficiency and syngas production, less amount of undesirable by-products, and longer lifetime of catalysts than that in the PPC process [35,206,207].

Obvious synergistic effect of DBD plasma and Ni/γ-Al_2O_3 catalyst was observed in the reforming of toluene as model tar compound [42]. Toluene conversion efficiency obtained a high value of 91.7% together with an energy efficiency of 16.8 g/kWh in the DBD plasma reactor coupled with Ni(5 wt%)/γ-Al_2O_3 catalyst [208]. In addition, tar is mainly converted to useful syngas with rare amount of coke formation in the plasma-catalysis system, while most carbon is transformed into soot during tar reforming in NTP without the addition of catalysts [134]. Lu et al. [209] concluded that the toluene was mainly converted via two pathways in a FeO_x/SBA-15 assisted DBD plasma system, i.e. (i) the direct decomposition of toluene in the gas phase caused by the collision of electrons; and (ii) the oxidation of toluene by the excited radicals (such as OH and O) on the catalyst surface. The Fe^{2+} in the FeO_x/SBA-15 catalyst played an important role in toluene decomposition due to its superior oxygen affinity. Besides, the outstanding adsorption ability of SBA-15 also contributed to the toluene conversion.

Liu et al [35] compared the steam reforming of toluene in three processes of PlO, PPC and IPC system. The IPC system with a Ni(3 wt %)/ZSM-5 catalyst exhibited much better performance than PlO and PPC system. Besides, the liquid byproduct species and mechanism of toluene reforming in IPC system was significantly different from that in PlO and PPC system, due to the interaction between short lifetime reactive plasma species (OH, O, O_2, etc.), and toluene and its intermediates. As shown in Fig. 19, the addition of Ni (3 wt.%)/ZSM-5 catalyst in the downstream of discharge zone of DBD plasma did not change the distribution of liquid byproducts compared to that in PlO system, since the short lifetime reactive plasma species cannot reach the catalysts in the downstream of DBD plasma. However, the interaction of DBD plasma and Ni (3 wt.%)/ZSM-5 catalyst contributed to an absolutely different species of byproducts with much less amount and species in IPC system.

Based on the above summarization, superior performance has been achieved for tar reforming in the IPC system, due to the synergistic effect of NTP and heterogeneous catalysts. However, the interaction between NTP and heterogeneous catalyst in an IPC process is much

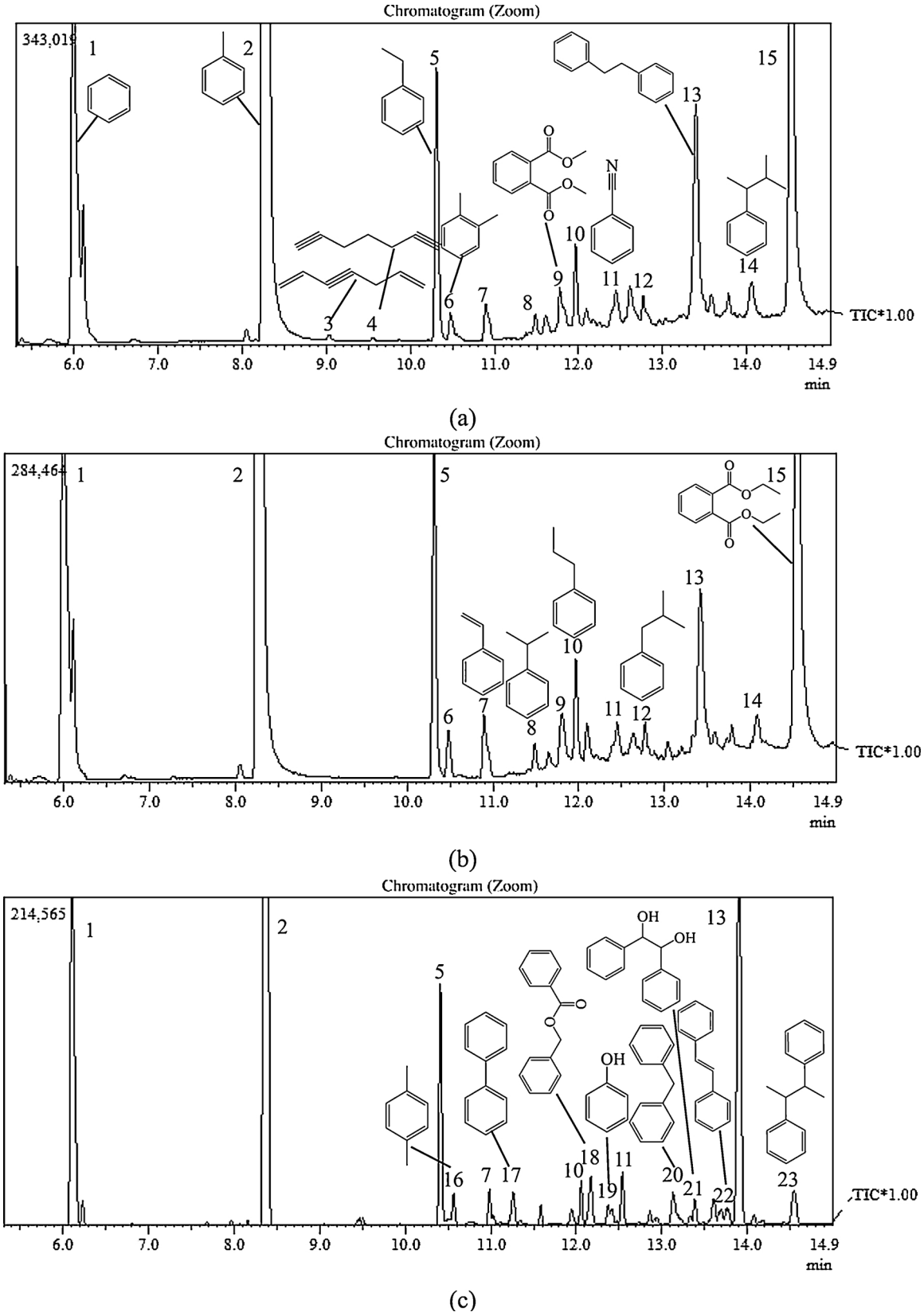

Fig. 19. GC–MS spectra of liquid byproducts during steam reforming of toluene in the (a) PlO, (b) PPC and (c) IPC systems [35].

more complex compared with the PPC process [210]. On one hand, the produced short lifetime reactive plasma species could influence the morphology and work function of catalyst [211,212]. On the other hand, the discharge characteristics are changed by the addition of catalysts in the discharge zone [210]. Lots of efforts have been made for the clarification of their synergistic effect, which will be further explained in this article.

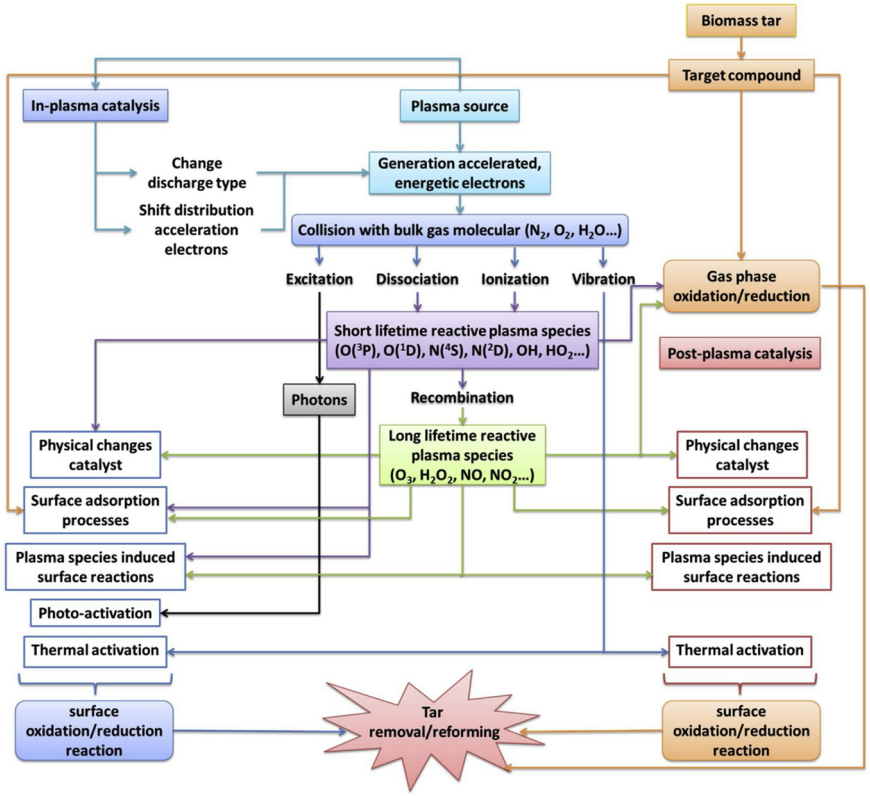

Fig. 20. Schematic of plasma-catalysis phenomena [181].

4.2. Synergistic effects of catalysts and plasma

The synergistic effect of NTP and heterogeneous catalysts is highly complicated. Fig. 20 summarizes different phenomena of IPC and PPC systems [181]. On one hand, the introduction of catalysts in plasma might influence the discharge type and the distribution of accelerated electrons, thereby affecting the formation of excited short lifetime reactive plasma species. New energetic species such as atomic oxygen, superoxide species (O_2^-), and hydroxyl radicals, can be produced in the IPC system in the presence of catalysts. Besides, more stable species, such as ozone and hydrogen peroxide, could also be generated by the combination of partial short lifetime reactive plasma species, which could reach the catalysts located in the downstream of the discharge zone (PPC). On the other hand, the presence of short lifetime and long lifetime reactive plasma species could cause the physical change of catalysts, and thus influence the surface adsorption of tar compounds. The plasma-catalysis reactions have been proven to be zero-order kinetics, indicating the importance of surface reaction in tar reforming. It can also be concluded from Fig. 20 that the increase of gas-phase temperature and the presence of photons both contribute to the activation of catalysts.

4.2.1. Effect of catalyst on non-thermal plasma

The addition of catalysts in the discharge zone of plasma can change the discharge type and the distribution of accelerated electrons [181,213]. The increased concentration of reactants in the discharge zone results in a more sufficient collision of reactants and excited species [214]. In addition, the microdischarge might occur in the pore structures of catalysts, leading to the increase of discharge in unit volume and the formation of new reactive species in the pores of catalysts [215].

For instance, the addition of a catalyst in the discharge zone of NTP triggered the polarization of catalysts and resulted in the accumulation of charge on the surface of catalyst. Therefore, the average electrical field was increased, as well as the number of energetic electrons and reactive species, which was determined by the enhancement of microdischarges around the contact points of catalysts [216,217]. Tu et al. [218] demonstrated that the intensity of current pulse of the hybrid plasma-catalysis reactor was increased by installing a Ni/γ-Al_2O_3 catalyst in DBD plasma. The addition of $BaTiO_3$ and TiO_2 photocatalysts led to an increase of the mean electric field and mean electron energy by 9–11% [219].

Furthermore, Holzer et al. [220] found that the energy input in a ferroelectric material-assisted NTP was 6˜10 times higher than that in a NTP without additives, which might be caused by the formation of strong microdischarges in the intra- and inter-pores of catalysts with a particle size of 1000 μm–5000 μm. Zhang et al. [210] investigated the microdischarge behavior inside the pore of catalysts located in the discharge zone of helium DBD plasma using a two-dimensional fluid model, since the formation of stable discharge in the pore of catalysts is of significant importance which determines the active surface for catalytic reactions. They predicted that a stable discharge could be generated in the pores with size of above 10 μm. The electron impact ionization preferentially occurred in the pore of catalysts due to the high electric field and electron temperature. The increase of pore size and applied voltage both contributed to the enhancement of ionization [221,222].

4.2.2. Effect of non-thermal plasma on catalyst

NTP shows multiple effects on the behaviors of catalysts in tar reforming, including changing the status of reactants and influencing the properties of catalysts, such as the morphology and work function of catalysts. Specially, the induced changes of catalysts are highly correlated [212]. For example, the electronic properties of catalyst can be modified by changing its morphology and thus changing its chemical properties.

The reactants can be transformed to different byproducts and intermediates in the presence of plasma, which are much easier to be

decomposed and reformed on the catalyst surface at lower temperatures [180]. Xu et al. [208] found that the introduction of DBD plasma in toluene reforming promoted the methanation reactions (reaction 46–47) of fuel gas in the catalytic process, which were favorable at higher temperatures. Tsodikov et al. [223] revealed that the presence of MW plasma in the catalytic reforming of lignin was beneficial to the cracking of C–H bonds, leading to the formation of syngas as the dominant products. However, a significant amount of C—C bonds were cracked in the convective heating process, giving rise to the formation of aromatic liquid byproducts.

$$CO + 3H_2 \rightarrow CH_4 + H_2O \quad (46)$$

$$CO_2 + 4H_2 \rightarrow CH_4 + 2H_2O \quad (47)$$

In addition, the properties of catalysts can also be enhanced in the presence of NTP, by changing the structural properties of catalysts (morphology, specific surface area, particle size and metal dispersion), generating short lifetime and long lifetime excited plasma species on the catalyst surface and improving the activity and stability of catalysts at room temperature and atmospheric pressure [224–226]. Previous studies showed that Pt/CeO_2 catalyst installed in the discharge zone of plasma exhibited larger specific surface area due to the generation of abundant notches on catalyst surface and broken CeO_2 nanorods under the plasma. In addition, smaller particle size, higher Pt dispersion and higher concentration of oxygen vacancies and Ce^{3+} were also observed. A stronger interaction of active metal and support material contributed to a lower reduction temperature. The properties of Pt/CeO_2 catalyst after plasma treatment resulted in higher toluene conversion efficiency and better catalyst stability [227]. Rahmani et al. [228] demonstrated that the application of ultrasonic plasma efficiently prevented the blocking of support mesopores and improved the adsorption properties of Pt/CeO_2–Al_2O_3 catalyst. A smaller particle size and better dispersion of Pt was obtained for the plasma treated catalyst, which can provide more active sites for toluene abatement. The stability of catalysts could also be modified by the introduction of NTP in the hybrid plasma-catalysis system [44]. Previous studies demonstrated that tar is mainly converted to useful syngas with rare amount of coke formation in a plasma-catalysis system [134], while abundant coke was deposited on the catalyst surface in the absence of NTP [64].

The hybrid NTP catalysis system has been widely applied in different aspects including the removal of air pollutants, hydrogen production and reforming of hydrocarbons [229–232]. However, further efforts are still essential for clarifying the synergist effect of NTP and heterogeneous catalysts in reforming of tar derived from biomass gasification. It is beneficial to the development and commercial application of the hybrid plasma-catalysis system for tar reforming and biomass gasification.

5. Future aspects

The hybrid plasma-catalysis technology is of significant potential in tar reforming due to the high tar conversion efficiency and selectivity of syngas. However, further improvements are still essential for its development and commercialization.

Firstly, model tar compounds, such as toluene, benzene, naphthalene, phenol, ect., were generally used for the steam reforming of tar in the hybrid NTP-catalysis system. However, the actual tar derived from biomass gasification was much more complex, since it contains aromatic hydrocarbons up to five rings, oxygenates and polycyclic aromatic hydrocarbons (PAHs). Therefore, the steam reforming of actual tar in the hybrid NTP-catalysis system or integrating biomass gasification in the NTP-catalysis system should be further investigated for the purpose of evaluating the performance of this system in industrial processes.

Secondly, the traditional Ni/γ-Al_2O_3 catalyst was the most widely used catalyst in the hybrid NTP-catalysis system, but it exhibited poor resistance to coke formation and sulfur poisoning. Therefore, the development of catalysts with higher activity and stability, and better resistance to coke deposition and sulfur poisoning should be developed to improve the performance of the hybrid system.

Thirdly, recent studies focused on the production of syngas in steam reforming of tar, since it can be used as secondary raw feedstock to produce synthesis fuels. In our opinion, the one-step synthesis of chemical fuels, including methanol, dimethylether (DME), ethanol and Fischer-Tropsch fuels, can be studied in the steam reforming of biomass tar by adjusting S/C ratio, optimizing reaction parameters, and selecting appropriate catalyst species.

6. Concluding remarks

This article reviews and compares the performance of tar reforming using catalysis-only, plasma-only and hybrid plasma-catalyst system. For the catalytic reforming, the deactivation of catalysts caused by poisoning, sintering and coke deposition is the main drawback. Besides, the catalytic reforming is generally operated at high temperatures, leading to high energy consumption. For the plasma reforming, tar can be decomposed efficiently in plasma reactor even at room temperature, but the uncontrollable byproduct and low syngas selectivity limit its development. Therefore, the combination of plasma and heterogeneous catalyst is considered to be a promising alternative for tar reforming, by generating a synergy effect.

The plasma and catalyst could be combined via the pretreatment of catalyst by plasma, locating the catalyst in the downstream of plasma reactor (PPC), and installing the catalyst in the discharge zone of plasma (IPC). The synergistic effect of plasma and catalyst can increase the tar conversion and syngas production, reduce the formation of undesirable liquid byproducts and coke deposition, and promote the catalytic activity and stability. The synergy of plasma and catalyst is a complex phenomenon, originating from the interactions between various plasma-catalysis processes. The addition of catalyst in plasma can change the discharge properties and shift the distribution of accelerated electrons, while the presence of plasma in the catalytic process leads to the changes of the reactant status, the modification of catalyst properties, including the structural properties and work function, and the exposure of excited plasma species on the catalyst surface.

Acknowledgements

The research is financially supported by National University of Singapore, National Environmental Agency (NEA-ETRP Grant RP No. 279-000-491-279), A*STAR (AME IRG 2017 Grant RP No. 279-000-509-305) and Ministry of Education (MOE T2 Grant RP No. 279-000-544-112).

References

[1] S. Heidenreich, P.U. Foscolo, New concepts in biomass gasification, Prog. Energy Combust. Sci. 46 (2015) 72–95.
[2] C.F. Palma, Modelling of tar formation and evolution for biomass gasification: a review, Appl. Energy 111 (2013) 129–141.
[3] Y. Shen, K. Yoshikawa, Recent progresses in catalytic tar elimination during biomass gasification or pyrolysis—a review, Renew. Sustain. Energy Rev. 21 (2013) 371–392.
[4] E.F. Iliopoulou, S. Stefanidis, K. Kalogiannis, A. Delimitis, A. Lappas, K. Triantafyllidis, Catalytic upgrading of biomass pyrolysis vapors using transition metal-modified ZSM-5 zeolite, Appl. Catal. B 127 (2012) 281–290.
[5] T. Kan, V. Strezov, T.J. Evans, Lignocellulosic biomass pyrolysis: a review of product properties and effects of pyrolysis parameters, Renew. Sustain. Energy Rev. 57 (2016) 1126–1140.
[6] A. Sharma, V. Pareek, D. Zhang, Biomass pyrolysis—a review of modelling, process parameters and catalytic studies, Renew. Sustain. Energy Rev. 50 (2015) 1081–1096.
[7] S.D. Stefanidis, K.G. Kalogiannis, E.F. Iliopoulou, C.M. Michailof, P.A. Pilavachi, A.A. Lappas, A study of lignocellulosic biomass pyrolysis via the pyrolysis of cellulose, hemicellulose and lignin, J. Anal. Appl. Pyrolysis 105 (2014) 143–150.
[8] S. Wang, G. Dai, H. Yang, Z. Luo, Lignocellulosic biomass pyrolysis mechanism: a

state-of-the-art review, Prog. Energy Combust. Sci. 62 (2017) 33–86.
[9] M. Shahbaz, A. Inayat, D.O. Patrick, M. Ammar, The influence of catalysts in biomass steam gasification and catalytic potential of coal bottom ash in biomass steam gasification: a review, Renew. Sustain. Energy Rev. 73 (2017) 468–476.
[10] C.A.V.B. de Sales, D.M.Y. Maya, E.E.S. Lora, R.L. Jaén, A.M.M. Reyes, A.M. González, R.V. Andrade, J.D. Martínez, Experimental study on biomass (eucalyptus spp.) gasification in a two-stage downdraft reactor by using mixtures of air, saturated steam and oxygen as gasifying agents, Energy Convers. Manage. 145 (2017) 314–323.
[11] S. Nizamuddin, H.A. Baloch, G. Griffin, N. Mubarak, A.W. Bhutto, R. Abro, S.A. Mazari, B.S. Ali, An overview of effect of process parameters on hydrothermal carbonization of biomass, Renew. Sustain. Energy Rev. 73 (2017) 1289–1299.
[12] M. Salimi, A. Tavasoli, S. Balou, H. Hashemi, K. Kohansal, Influence of promoted bimetallic Ni-based catalysts and micro/mesopores carbonaceous supports for biomass hydrothermal conversion to H_2-rich gas, Appl. Catal. B 239 (2018) 383–397.
[13] M. Huang, J. Luo, Z. Fang, H. Li, Biodiesel production catalyzed by highly acidic carbonaceous catalysts synthesized via carbonizing lignin in sub-and super-critical ethanol, Appl. Catal. B 190 (2016) 103–114.
[14] D. Chen, Z. Zheng, K. Fu, Z. Zeng, J. Wang, M. Lu, Torrefaction of biomass stalk and its effect on the yield and quality of pyrolysis products, Fuel 159 (2015) 27–32.
[15] S. Neupane, S. Adhikari, Z. Wang, A. Ragauskas, Y. Pu, Effect of torrefaction on biomass structure and hydrocarbon production from fast pyrolysis, Green Chem. 17 (2015) 2406–2417.
[16] Y. Chen, H. Yang, Q. Yang, H. Hao, B. Zhu, H. Chen, Torrefaction of agriculture straws and its application on biomass pyrolysis poly-generation, Bioresour. Technol. 156 (2014) 70–77.
[17] Y. Shen, P. Zhao, Q. Shao, D. Ma, F. Takahashi, K. Yoshikawa, In-situ catalytic conversion of tar using rice husk char-supported nickel-iron catalysts for biomass pyrolysis/gasification, Appl. Catal. B 152 (2014) 140–151.
[18] Z. Zhang, L. Liu, B. Shen, C. Wu, Preparation, modification and development of Ni-based catalysts for catalytic reforming of tar produced from biomass gasification, Renewable Sustainable Energy Rev. 94 (2018) 1086–1109.
[19] P.J. Woolcock, R.C. Brown, A review of cleaning technologies for biomass-derived syngas, Biomass Bioenergy 52 (2013) 54–84.
[20] S. Sartipi, K. Parashar, M.J. Valero-Romero, V.P. Santos, B. van der Linden, M. Makkee, F. Kapteijn, J. Gascon, Hierarchical H-ZSM-5-supported cobalt for the direct synthesis of gasoline-range hydrocarbons from syngas: advantages, limitations, and mechanistic insight, J. Catal. 305 (2013) 179–190.
[21] Y. Shen, Chars as carbonaceous adsorbents/catalysts for tar elimination during biomass pyrolysis or gasification, Renew. Sustain. Energy Rev. 43 (2015) 281–295.
[22] F. García-Labiano, P. Gayán, L. De Diego, A. Abad, T. Mendiara, J. Adánez, M. Nacken, S. Heidenreich, Tar abatement in a fixed bed catalytic filter candle during biomass gasification in a dual fluidized bed, Appl. Catal. B 188 (2016) 198–206.
[23] M. Wnukowski, P. Jamroz, Microwave plasma treatment of simulated biomass syngas: interactions between the permanent syngas compounds and their influence on the model tar compound conversion, Fuel Process. Technol. 173 (2018) 229–242.
[24] M. Asadullah, Biomass gasification gas cleaning for downstream applications: a comparative critical review, Renewable Sustainable Energy Rev. 40 (2014) 118–132.
[25] A.F. Kirkels, G.P. Verbong, Biomass gasification: still promising? A 30-year global overview, Renew. Sustain. Energy Rev. 15 (2011) 471–481.
[26] P. Knutsson, V. Cantatore, M. Seemann, P.L. Tam, I. Panas, Role of potassium in the enhancement of the catalytic activity of calcium oxide towards tar reduction, Appl. Catal. B 229 (2018) 88–95.
[27] A.S. Al-Rahbi, P.T. Williams, Hydrogen-rich syngas production and tar removal from biomass gasification using sacrificial tyre pyrolysis char, Appl. Energy 190 (2017) 501–509.
[28] G. Guan, M. Kaewpanha, X. Hao, A. Abudula, Catalytic steam reforming of biomass tar: prospects and challenges, Renew. Sustain. Energy Rev. 58 (2016) 450–461.
[29] A. Bhave, D. Vyas, J. Patel, A wet packed bed scrubber-based producer gas cooling–cleaning system, Renew. Energy 33 (2008) 1716–1720.
[30] M. Ni, D.Y. Leung, M.K. Leung, K. Sumathy, An overview of hydrogen production from biomass, Fuel Process. Technol. 87 (2006) 461–472.
[31] C. Zuber, C. Hochenauer, T. Kienberger, Test of a hydrodesulfurization catalyst in a biomass tar removal process with catalytic steam reforming, Appl. Catal. B 156 (2014) 62–71.
[32] M. Virginie, J. Adánez, C. Courson, L. De Diego, F. García-Labiano, D. Niznansky, A. Kiennemann, P. Gayán, A. Abad, Effect of Fe–olivine on the tar content during biomass gasification in a dual fluidized bed, Appl. Catal. B 121 (2012) 214–222.
[33] S. Liu, D. Mei, L. Wang, X. Tu, Steam reforming of toluene as biomass tar model compound in a gliding arc discharge reactor, Chem. Eng. J. 307 (2017) 793–802.
[34] L. Liu, Q. Wang, S. Ahmad, X. Yang, M. Ji, Y. Sun, Steam reforming of toluene as model biomass tar to H_2-rich syngas in a DBD plasma-catalytic system, J. Energy Inst. 91 (2018) 929–939.
[35] L. Liu, Q. Wang, J. Song, S. Ahmad, X. Yang, Y. Sun, Plasma-assisted catalytic reforming of toluene to hydrogen rich syngas, Catal. Sci. Technol. 7 (2017) 4216–4231.
[36] D. Li, M. Tamura, Y. Nakagawa, K. Tomishige, Metal catalysts for steam reforming of tar derived from the gasification of lignocellulosic biomass, Bioresour. Technol. 178 (2015) 53–64.
[37] Y. Chen, Y.-h. Luo, W.-g. Wu, Y. Su, Experimental investigation on tar formation and destruction in a lab-scale two-stage reactor, Energy Fuels 23 (2009) 4659–4667.
[38] S. Zhang, Y. Song, Y.C. Song, Q. Yi, L. Dong, T.T. Li, L. Zhang, J. Feng, W.Y. Li, C.-Z. Li, An advanced biomass gasification technology with integrated catalytic hot gas cleaning. Part III: Effects of inorganic species in char on the reforming of tars from wood and agricultural wastes, Fuel 183 (2016) 177–184.
[39] A. Ochoa, A. Arregi, M. Amutio, A.G. Gayubo, M. Olazar, J. Bilbao, P. Castaño, Coking and sintering progress of a Ni supported catalyst in the steam reforming of biomass pyrolysis volatiles, Appl. Catal. B 233 (2018) 289–300.
[40] P. Jamróz, W. Kordylewski, M. Wnukowski, Microwave plasma application in decomposition and steam reforming of model tar compounds, Fuel Process. Technol. 169 (2018) 1–14.
[41] X. Zhu, S. Zhang, Y. Yang, C. Zheng, J. Zhou, X. Gao, X. Tu, Enhanced performance for plasma-catalytic oxidation of ethyl acetate over $La_{1-x}Ce_xCoO_{3+\delta}$ catalysts, Appl. Catal. B 213 (2017) 97–105.
[42] S. Liu, D. Mei, M. Nahil, S. Gadkari, S. Gu, P. Williams, X. Tu, Hybrid plasma-catalytic steam reforming of toluene as a biomass tar model compound over Ni/Al_2O_3 catalysts, Fuel Process. Technol. 166 (2017) 269–275.
[43] X. Zhu, X. Gao, R. Qin, Y. Zeng, R. Qu, C. Zheng, X. Tu, Plasma-catalytic removal of formaldehyde over Cu–Ce catalysts in a dielectric barrier discharge reactor, Appl. Catal. B 170 (2015) 293–300.
[44] W.-C. Chung, M.-B. Chang, Review of catalysis and plasma performance on dry reforming of CH_4 and possible synergistic effects, Renew. Sustain. Energy Rev. 62 (2016) 13–31.
[45] S. Delagrange, L. Pinard, J.-M. Tatibouët, Combination of a non-thermal plasma and a catalyst for toluene removal from air: manganese based oxide catalysts, Appl. Catal. B 68 (2006) 92–98.
[46] M.L.V. Rios, A.M. González, E.E.S. Lora, O.A.A. del Olmo, Reduction of tar generated during biomass gasification: a review, Biomass Bioenergy 108 (2018) 345–370.
[47] Y. Shen, J. Wang, X. Ge, M. Chen, By-products recycling for syngas cleanup in biomass pyrolysis–an overview, Renew. Sustain. Energy Rev. 59 (2016) 1246–1268.
[48] S. Anis, Z. Zainal, Tar reduction in biomass producer gas via mechanical, catalytic and thermal methods: a review, Renew. Sustain. Energy Rev. 15 (2011) 2355–2377.
[49] H. De Lasa, E. Salaices, J. Mazumder, R. Lucky, Catalytic steam gasification of biomass: catalysts, thermodynamics and kinetics, Chem. Rev. 111 (2011) 5404–5433.
[50] Y. Richardson, J. Blin, A. Julbe, A short overview on purification and conditioning of syngas produced by biomass gasification: catalytic strategies, process intensification and new concepts, Prog. Energy Combust. Sci. 38 (2012) 765–781.
[51] S.Y. Park, G. Oh, K. Kim, M.W. Seo, H.W. Ra, T.Y. Mun, J.G. Lee, S.J. Yoon, Deactivation characteristics of Ni and Ru catalysts in tar steam reforming, Renew. Energy 105 (2017) 76–83.
[52] P.H. Moud, K.J. Andersson, R. Lanza, K. Engvall, Equilibrium potassium coverage and its effect on a Ni tar reforming catalyst in alkali-and sulfur-laden biomass gasification gases, Appl. Catal. B 190 (2016) 137–146.
[53] D. Laprune, C. Theodoridi, A. Tuel, D. Farrusseng, F. Meunier, Effect of polyaromatic tars on the activity for methane steam reforming of nickel particles embedded in silicalite-1, Appl. Catal. B 204 (2017) 515–524.
[54] I. Zamboni, C. Courson, A. Kiennemann, Fe-Ca interactions in Fe-based/CaO catalyst/sorbent for CO_2 sorption and hydrogen production from toluene steam reforming, Appl. Catal. B 203 (2017) 154–165.
[55] L. Wang, Y. Hisada, M. Koike, D. Li, H. Watanabe, Y. Nakagawa, K. Tomishige, Catalyst property of Co–Fe alloy particles in the steam reforming of biomass tar and toluene, Appl. Catal. B 121 (2012) 95–104.
[56] J. Meng, Z. Zhao, X. Wang, A. Zheng, D. Zhang, Z. Huang, K. Zhao, G. Wei, H. Li, Comparative study on phenol and naphthalene steam reforming over Ni-Fe alloy catalysts supported on olivine synthesized by different methods, Energy Convers. Manage. 168 (2018) 60–73.
[57] D.A. Constantinou, J.L.G. Fierro, A.M. Efstathiou, A comparative study of the steam reforming of phenol towards H_2 production over natural calcite, dolomite and olivine materials, Appl. Catal. B 95 (2010) 255–269.
[58] M. Zhao, T.L. Church, A.T. Harris, SBA-15 supported Ni-Co bimetallic catalysts for enhanced hydrogen production during cellulose decomposition, Appl. Catal. B 101 (2011) 522–530.
[59] Y. Shen, P. Zhao, Q. Shao, F. Takahashi, K. Yoshikawa, In situ catalytic conversion of tar using rice husk char/ash supported nickel–iron catalysts for biomass pyrolytic gasification combined with the mixing-simulation in fluidized-bed gasifier, Appl. Energy 160 (2015) 808–819.
[60] F. Guo, X. Li, Y. Liu, K. Peng, C. Guo, Z. Rao, Catalytic cracking of biomass pyrolysis tar over char-supported catalysts, Energy Convers. Manage. 167 (2018) 81–90.
[61] J. Chen, M. Tamura, Y. Nakagawa, K. Okumura, K. Tomishige, Promoting effect of trace Pd on hydrotalcite-derived Ni/Mg/Al catalyst in oxidative steam reforming of biomass tar, Appl. Catal. B 179 (2015) 412–421.
[62] D. Li, L. Wang, M. Koike, Y. Nakagawa, K. Tomishige, Steam reforming of tar from pyrolysis of biomass over Ni/Mg/Al catalysts prepared from hydrotalcite-like precursors, Appl. Catal. B 102 (2011) 528–538.
[63] D. Świerczyński, S. Libs, C. Courson, A. Kiennemann, Steam reforming of tar from a biomass gasification process over Ni/olivine catalyst using toluene as a model compound, Appl. Catal. B 74 (2007) 211–222.
[64] J. Cao, J. Ren, X. Zhao, X. Wei, T. Takarada, Effect of atmosphere on carbon deposition of Ni/Al_2O_3 and Ni-loaded on lignite char during reforming of toluene as a biomass tar model compound, Fuel 217 (2018) 515–521.

[65] T. Mendiara, J.M. Johansen, R. Utrilla, A.D. Jensen, P. Glarborg, Evaluation of different oxygen carriers for biomass tar reforming (II): carbon deposition in experiments with methane and other gases, Fuel 90 (2011) 1370–1382.

[66] T. Miyazawa, T. Kimura, J. Nishikawa, S. Kado, K. Kunimori, K. Tomishige, Catalytic performance of supported Ni catalysts in partial oxidation and steam reforming of tar derived from the pyrolysis of wood biomass, Catal. Today 115 (2006) 254–262.

[67] M. Kong, J. Fei, S. Wang, W. Lu, X. Zheng, Influence of supports on catalytic behavior of nickel catalysts in carbon dioxide reforming of toluene as a model compound of tar from biomass gasification, Bioresour. Technol. 102 (2011) 2004–2008.

[68] M. Koike, D. Li, H. Watanabe, Y. Nakagawa, K. Tomishige, Comparative study on steam reforming of model aromatic compounds of biomass tar over Ni and Ni–Fe alloy nanoparticles, Appl. Catal. A Gen. 506 (2015) 151–162.

[69] J. Ashok, S. Kawi, Steam reforming of biomass tar model compound at relatively low steam-to-carbon condition over CaO-doped nickel–iron alloy supported over iron–alumina catalysts, Appl. Catal. A Gen. 490 (2015) 24–35.

[70] J.-P. Cao, P. Shi, X.-Y. Zhao, X.-Y. Wei, T. Takarada, Catalytic reforming of volatiles and nitrogen compounds from sewage sludge pyrolysis to clean hydrogen and synthetic gas over a nickel catalyst, Fuel Process. Technol. 123 (2014) 34–40.

[71] M. Artetxe, J. Alvarez, M.A. Nahil, M. Olazar, P.T. Williams, Steam reforming of different biomass tar model compounds over Ni/Al_2O_3 catalysts, Energy Convers. Manage. 136 (2017) 119–126.

[72] M.M. Yung, J.N. Kuhn, Deactivation mechanisms of Ni-based tar reforming catalysts as monitored by X-ray absorption spectroscopy, Langmuir 26 (2010) 16589–16594.

[73] I.E. Achouri, N. Abatzoglou, C. Fauteux-Lefebvre, N. Braidy, Diesel steam reforming: comparison of two nickel aluminate catalysts prepared by wet-impregnation and co-precipitation, Catal. Today 207 (2013) 13–20.

[74] J. Ashok, S. Kawi, Nickel–iron alloy supported over iron–alumina catalysts for steam reforming of biomass tar model compound, ACS Catal. 4 (2013) 289–301.

[75] J. Ashok, Y. Kathiraser, M. Ang, S. Kawi, Ni and/or Ni–Cu alloys supported over SiO_2 catalysts synthesized via phyllosilicate structures for steam reforming of biomass tar reaction, Catal. Sci. Technol. 5 (2015) 4398–4409.

[76] D. Harshini, D.H. Lee, J. Jeong, Y. Kim, S.W. Nam, H.C. Ham, J.H. Han, T.-H. Lim, C.W. Yoon, Enhanced oxygen storage capacity of Ce0. $65Hf_{0.25}M_{0.1}O_{2-\delta}$ (M= rare earth elements): applications to methane steam reforming with high coking resistance, Appl. Catal. B 148 (2014) 415–423.

[77] M. Muñoz, S. Moreno, R. Molina, Promoter effect of Ce and Pr on the catalytic stability of the Ni-Co system for the oxidative steam reforming of ethanol, Appl. Catal. A Gen. 526 (2016) 84–94.

[78] F. Chen, C. Wu, L. Dong, A. Vassallo, P.T. Williams, J. Huang, Characteristics and catalytic properties of $Ni/CaAlO_x$ catalyst for hydrogen-enriched syngas production from pyrolysis-steam reforming of biomass sawdust, Appl. Catal. B 183 (2016) 168–175.

[79] L. Santamaria, G. Lopez, A. Arregi, M. Amutio, M. Artetxe, J. Bilbao, M. Olazar, Influence of the support on Ni catalysts performance in the in-line steam reforming of biomass fast pyrolysis derived volatiles, Appl. Catal. B 229 (2018) 105–113.

[80] H. Wang, J.T. Miller, M. Shakouri, C. Xi, T. Wu, H. Zhao, M.C. Akatay, XANES and EXAFS studies on metal nanoparticle growth and bimetallic interaction of Ni-based catalysts for CO_2 reforming of CH_4, Catal. Today 207 (2013) 3–12.

[81] D.H. Heo, R. Lee, J.H. Hwang, J.M. Sohn, The effect of addition of Ca, K and Mn over Ni-based catalyst on steam reforming of toluene as model tar compound, Catal. Today 265 (2016) 95–102.

[82] M.M. Yung, W.S. Jablonski, K.A. Magrini-Bair, Review of catalytic conditioning of biomass-derived syngas, Energy Fuels 23 (2009) 1874–1887.

[83] M. Virginie, C. Courson, D. Niznansky, N. Chaoui, A. Kiennemann, Characterization and reactivity in toluene reforming of a Fe/olivine catalyst designed for gas cleanup in biomass gasification, Appl. Catal. B 101 (2010) 90–100.

[84] A. Laobuthee, C. Veranitisagul, W. Wattanathana, N. Koonsaeng, N. Laosiripojana, Activity of Fe supported by $Ce_{1-x}Sm_xO_{2-\delta}$ derived from metal complex decomposition toward the steam reforming of toluene as biomass tar model compound, Renew. Energy 74 (2015) 133–138.

[85] J. Yu, F.-J. Tian, L. McKenzie, C.-Z. Li, Char-supported nano iron catalyst for water-gas-shift reaction: hydrogen production from coal/biomass gasification, Process. Saf. Environ. Prot. 84 (2006) 125–130.

[86] D. Laprune, D. Farrusseng, Y. Schuurman, F. Meunier, J. Pieterse, A. Steele, S. Thorpe, Effects of H_2S and phenanthrene on the activity of Ni and Rh-based catalysts for the reforming of a simulated biomass-derived producer gas, Appl. Catal. B 221 (2018) 206–214.

[87] T. Miyazawa, T. Kimura, J. Nishikawa, K. Kunimori, K. Tomishige, Catalytic properties of $Rh/CeO_2/SiO_2$ for synthesis gas production from biomass by catalytic partial oxidation of tar, Sci. Technol. Adv. Mater. 6 (2005) 604–614.

[88] G. Oh, S.Y. Park, M.W. Seo, Y.K. Kim, H.W. Ra, J.-G. Lee, S.J. Yoon, Ni/Ru–Mn/Al_2O_3 catalysts for steam reforming of toluene as model biomass tar, Renew. Energy 86 (2016) 841–847.

[89] F. Morales-Cano, L.F. Lundegaard, R.R. Tiruvalam, H. Falsig, M.S. Skjøth-Rasmussen, Improving the sintering resistance of Ni/Al_2O_3 steam-reforming catalysts by promotion with noble metals, Appl. Catal. A Gen. 498 (2015) 117–125.

[90] D. Mei, V.-A. Glezakou, V. Lebarbier, L. Kovarik, H. Wan, K.O. Albrecht, M. Gerber, R. Rousseau, R.A. Dagle, Highly active and stable $MgAl_2O_4$-supported Rh and Ir catalysts for methane steam reforming: a combined experimental and theoretical study, J. Catal. 316 (2014) 11–23.

[91] X. Zou, T. Chen, P. Zhang, D. Chen, J. He, Y. Dang, Z. Ma, Y. Chen, P. Toloueinia, C. Zhu, High catalytic performance of Fe-Ni/Palygorskite in the steam reforming of toluene for hydrogen production, Appl. Energy 226 (2018) 827–837.

[92] J. Ashok, S. Kawi, Steam reforming of toluene as a biomass tar model compound over CeO_2 promoted $Ni/CaO–Al_2O_3$ catalytic systems, Int. J. Hydrogen Energy 38 (2013) 13938–13949.

[93] L. Jiang, S. Hu, Y. Wang, S. Su, L. Sun, B. Xu, L. He, J. Xiang, Catalytic effects of inherent alkali and alkaline earth metallic species on steam gasification of biomass, Int. J. Hydrogen Energy 40 (2015) 15460–15469.

[94] U. Oemar, M.L. Ang, W.F. Hee, K. Hidajat, S. Kawi, Perovskite $La_xM_{1-x}Ni_{0.8}Fe_{0.2}O_3$catalyst for steam reforming of toluene: crucial role of alkaline earth metal at low steam condition, Appl. Catal. B: Environ. 148–149 (2014) 231–242.

[95] D. Feng, Y. Zhao, Y. Zhang, S. Sun, S. Meng, Y. Guo, Y. Huang, Effects of K and Ca on reforming of model tar compounds with pyrolysis biochars under H_2O or CO_2, Chem. Eng. J. 306 (2016) 422–432.

[96] D. Harshini, D.H. Lee, J. Jeong, Y. Kim, S.W. Nam, H.C. Ham, J.H. Han, T.H. Lim, W.Y. Chang, D. Harshini, Enhanced oxygen storage capacity of $Ce_{0.65}Hf_{0.25}M_{0.1}O_{2-\delta}$ (M = rare earth elements): applications to methane steam reforming with high coking resistance, Appl. Catal. B 148-149 (2014) 415–423.

[97] J. Tao, L.Q. Zhao, C.Q. Dong, L. Qiang, X.Z. Du, E. Dahlquist, Catalytic steam reforming of toluene as a model compound of biomass gasification tar using Ni-CeO_2/SBA-15 catalysts, Energies 6 (2013) 3284–3296.

[98] R. Zhang, H. Wang, X. Hou, Catalytic reforming of toluene as tar model compound: effect of Ce and Ce-Mg promoter using Ni/olivine catalyst, Chemosphere 97 (2014) 40–46.

[99] B. Jiang, L. Li, Z. Bian, Z. Li, M. Othman, Z. Sun, D. Tang, S. Kawi, B. Dou, Hydrogen generation from chemical looping reforming of glycerol by Ce-doped nickel phyllosilicate nanotube oxygen carriers, Fuel 222 (2018) 185–192.

[100] U. Oemar, Y. Kathiraser, M.L. Ang, K. Hidajat, S. Kawi, Catalytic biomass gasification to syngas over highly dispersed lanthanum-doped nickel on SBA-15, ChemCatChem 7 (2015) 3376–3385.

[101] U. Oemar, M.L. Ang, Y.C. Chin, K. Hidajat, S. Kawi, Role of lattice oxygen in oxidative steam reforming of toluene as a tar model compound over Ni/$La_{0.8}Sr_{0.2}AlO_3$ catalyst, Catal. Sci. Technol. 5 (2015) 3585–3597.

[102] L.-x. Zhang, T. Matsuhara, S. Kudo, J.-i. Hayashi, K. Norinaga, Rapid pyrolysis of brown coal in a drop-tube reactor with co-feeding of char as a promoter of in situ tar reforming, Fuel 112 (2013) 681–686.

[103] K. Seung-hoon, J. Jae-sun, Y. Eun-hyeok, L. Kwan-Young, M.D. Ju, Hydrogen production by steam reforming of biomass-derived glycerol over Ni-based catalysts, Catal. Today 228 (2014) 145–151.

[104] M. Qiu, Y. Li, T. Wang, Q. Zhang, C. Wang, X. Zhang, C. Wu, L. Ma, K. Li, Upgrading biomass fuel gas by reforming over Ni–MgO/γ-Al_2O_3 cordierite monolithic catalysts in the lab-scale reactor and pilot-scale multi-tube reformer, Appl. Energy 90 (2012) 3–10.

[105] G. Wu, C. Zhang, S. Li, Z. Han, T. Wang, X. Ma, J. Gong, Hydrogen production via glycerol steam reforming over Ni/Al_2O_3: influence of nickel precursors, ACS Sustain. Chem. Eng. 1 (2013) 1052–1062.

[106] D. Li, M. Koike, J. Chen, Y. Nakagawa, K. Tomishige, Preparation of Ni–Cu/Mg/Al catalysts from hydrotalcite-like compounds for hydrogen production by steam reforming of biomass tar, Int. J. Hydrogen Energy 39 (2014) 10959–10970.

[107] J. Ashok, Y. Kathiraser, M. Ang, S. Kawi, Bi-functional hydrotalcite-derived NiO–CaO–Al_2O_3 catalysts for steam reforming of biomass and/or tar model compound at low steam-to-carbon conditions, Appl. Catal. B 172 (2015) 116–128.

[108] G.-Y. Chen, C. Liu, W.-C. Ma, B.-B. Yan, N. Ji, Catalytic cracking of tar from biomass gasification over a HZSM-5-supported Ni–MgO catalyst, Energy Fuels 29 (2015) 7969–7974.

[109] S. Karnjanakom, G. Guan, B. Asep, X. Du, X. Hao, C. Samart, A. Abudula, Catalytic steam reforming of tar derived from steam gasification of sunflower stalk over ethylene glycol assisting prepared Ni/MCM-41, Energy Convers. Manage. 98 (2015) 359–368.

[110] T. Ahmed, S. Xiu, L. Wang, A. Shahbazi, Investigation of Ni/Fe/Mg zeolite-supported catalysts in steam reforming of tar using simulated-toluene as model compound, Fuel 211 (2018) 566–571.

[111] C. Wu, L. Wang, P.T. Williams, J. Shi, J. Huang, Hydrogen production from biomass gasification with Ni/MCM-41 catalysts: influence of Ni content, Appl. Catal. B 108 (2011) 6–13.

[112] E. Savuto, R. Navarro, N. Mota, A. Di Carlo, E. Bocci, M. Carlini, J. Fierro, Steam reforming of tar model compounds over Ni/Mayenite catalysts: effect of Ce addition, Fuel 224 (2018) 676–686.

[113] U. Oemar, P. Ang, K. Hidajat, S. Kawi, Promotional effect of Fe on perovskite $LaNi_xFe_{1-x}O_3$ catalyst for hydrogen production via steam reforming of toluene, Int. J. Hydrogen Energy 38 (2013) 5525–5534.

[114] J. Ashok, S. Das, N. Dewangan, S. Kawi, H_2S and NO_x tolerance capability of CeO_2 doped $La_{1-x}Ce_xCo_{0.5}Ti_{0.5}O_{3-\delta}$ perovskites for steam reforming of biomass tar model reaction, Energy Convers. Manage.: X (2019) 100003.

[115] Y. Shen, M. Chen, T. Sun, J. Jia, Catalytic reforming of pyrolysis tar over metallic nickel nanoparticles embedded in pyrochar, Fuel 159 (2015) 570–579.

[116] D. Feng, Y. Zhao, Y. Zhang, Z. Zhang, L. Zhang, S. Sun, In-situ steam reforming of biomass tar over sawdust biochar in mild catalytic temperature, Biomass Bioenergy 107 (2017) 261–270.

[117] S. Zhang, Z. Chen, H. Zhang, Y. Wang, X. Xu, L. Cheng, Y. Zhang, The catalytic reforming of tar from pyrolysis and gasification of brown coal: effects of parental carbon materials on the performance of char catalysts, Fuel Process. Technol. 174 (2018) 142–148.

[118] B. Lu, K. Kawamoto, Preparation of the highly loaded and well-dispersed NiO/SBA-15 for methanation of producer gas, Fuel 103 (2013) 699–704.

[119] Y. Kathiraser, J. Ashok, S. Kawi, Synthesis and evaluation of highly dispersed SBA-15 supported Ni–Fe bimetallic catalysts for steam reforming of biomass derived tar

reaction, Catal. Sci. Technol. 6 (2016) 4327–4336.
[120] K. Wang, B. Dou, B. Jiang, Q. Zhang, M. Li, H. Chen, Y. Xu, Effect of support on hydrogen production from chemical looping steam reforming of ethanol over Ni-based oxygen carriers, Int. J. Hydrogen Energy 41 (2016) 17334–17347.
[121] C.C. Xu, J. Donald, E. Byambajav, Y. Ohtsuka, Recent advances in catalysts for hot-gas removal of tar and NH_3 from biomass gasification, Fuel 89 (2010) 1784–1795.
[122] M. Kaewpanha, G. Guan, Y. Ma, X. Hao, Z. Zhang, P. Reubroychareon, K. Kusakabe, A. Abudula, Hydrogen production by steam reforming of biomass tar over biomass char supported molybdenum carbide catalyst, Int. J. Hydrogen Energy 40 (2015) 7974–7982.
[123] U. Oemar, M.L. Ang, K. Hidajat, S. Kawi, Enhancing performance of Ni/La_2O_3 catalyst by Sr-modification for steam reforming of toluene as model compound of biomass tar, RSC Adv. 5 (2015) 17834–17842.
[124] D. Yao, H. Yang, H. Chen, P.T. Williams, Co-precipitation, impregnation and so-gel preparation of Ni catalysts for pyrolysis-catalytic steam reforming of waste plastics, Appl. Catal. B 239 (2018) 565–577.
[125] X. Luo, Y. Hong, F. Wang, S. Hao, C. Pang, E. Lester, T. Wu, Development of nano Ni_xMg_yO solid solutions with outstanding anti-carbon deposition capability for the steam reforming of methanol, Appl. Catal. B 194 (2016) 84–97.
[126] C. Li, K. Suzuki, Tar property, analysis, reforming mechanism and model for biomass gasification—an overview, Renew. Sustain. Energy Rev. 13 (2009) 594–604.
[127] A. Jess, Mechanisms and kinetics of thermal reactions of aromatic hydrocarbons from pyrolysis of solid fuels, Fuel 75 (1996) 1441–1448.
[128] M. Artetxe, M.A. Nahil, M. Olazar, P.T. Williams, Steam reforming of phenol as biomass tar model compound over Ni/Al_2O_3 catalyst, Fuel 184 (2016) 629–636.
[129] U. Oemar, A. Ming Li, K. Hidajat, S. Kawi, Mechanism and kinetic modeling for steam reforming of toluene on La0. $8Sr_{0.2}Ni0.8Fe_{0.2}O_3$ catalyst, Aiche J. 60 (2014) 4190–4198.
[130] F. Saleem, K. Zhang, A. Harvey, Plasma-assisted decomposition of a biomass gasification tar analogue into lower hydrocarbons in a synthetic product gas using a dielectric barrier discharge reactor, Fuel 235 (2019) 1412–1419.
[131] S. Liu, D. Mei, Z. Shen, X. Tu, Nonoxidative conversion of methane in a dielectric barrier discharge reactor: prediction of reaction performance based on neural network model, J. Phys. Chem. C 118 (2014) 10686–10693.
[132] G. Petitpas, J.-D. Rollier, A. Darmon, J. Gonzalez-Aguilar, R. Metkemeijer, L. Fulcheri, A comparative study of non-thermal plasma assisted reforming technologies, Int. J. Hydrogen Energy 32 (2007) 2848–2867.
[133] K. Tao, N. Ohta, G. Liu, Y. Yoneyama, T. Wang, N. Tsubaki, Plasma enhanced catalytic reforming of biomass tar model compound to syngas, Fuel 104 (2013) 53–57.
[134] J. Sun, Q. Wang, W. Wang, K. Wang, Plasma catalytic steam reforming of a model tar compound by microwave-metal discharges, Fuel 234 (2018) 1278–1284.
[135] S. Nair, A. Pemen, K. Yan, F. Van Gompel, H. Van Leuken, E. Van Heesch, K. Ptasinski, A. Drinkenburg, Tar removal from biomass-derived fuel gas by pulsed corona discharges, Fuel Process. Technol. 84 (2003) 161–173.
[136] Y. Zeng, X. Zhu, D. Mei, B. Ashford, X. Tu, Plasma-catalytic dry reforming of methane over γ-Al_2O_3 supported metal catalysts, Catal. Today 256 (2015) 80–87.
[137] L. Liu, Q. Wang, S. Ahmad, X. Yang, M. Ji, Y. Sun, Steam reforming of toluene as model biomass tar to H2-rich syngas in a DBD plasma-catalytic system, J. Energy Inst. 91 (2018) 927–939.
[138] W. Mista, R. Kacprzyk, Decomposition of toluene using non-thermal plasma reactor at room temperature, Catal. Today 137 (2008) 345–349.
[139] F. Zhu, X. Li, H. Zhang, A. Wu, J. Yan, M. Ni, H. Zhang, A. Buekens, Destruction of toluene by rotating gliding arc discharge, Fuel 176 (2016) 78–85.
[140] Y.N. Chun, S.C. Kim, K. Yoshikawa, Decomposition of benzene as a surrogate tar in a gliding arc plasma, Environ. Prog. Sustain. Energy 32 (2013) 837–845.
[141] L. Yu, X. Li, X. Tu, Y. Wang, S. Lu, J. Yan, Decomposition of naphthalene by dc gliding arc gas discharge, J. Phys. Chem. A 114 (2009) 360–368.
[142] Y.C. Yang, Y.N. Chun, Naphthalene destruction performance from tar model compound using a gliding arc plasma reformer, Korean J. Chem. Eng. 28 (2011) 539–543.
[143] L. Liu, Q. Wang, J. Song, X. Yang, Y. Sun, Dry reforming of model biomass pyrolysis products to syngas by dielectric barrier discharge plasma, Int. J. Hydrogen Energy 43 (2018) 10281–10293.
[144] M. Hübner, R. Brandenburg, Y. Neubauer, J. Röpcke, On the reduction of gas--phase naphthalene using char–particles in a packed–bed atmospheric pressure plasma, Contrib. Plasma Phys. 55 (2015) 747–752.
[145] F. Saleem, K. Zhang, A. Harvey, Temperature dependence of non-thermal plasma assisted hydrocracking of toluene to lower hydrocarbons in a dielectric barrier discharge reactor, Chem. Eng. J. 356 (2019) 1062–1069.
[146] R.M. Eliott, M.F. Nogueira, A.S. Silva Sobrinho, B.A. Couto, H.S. Maciel, P.T. Lacava, Tar reforming under a microwave plasma torch, Energy Fuels 27 (2013) 1174–1181.
[147] M. Materazzi, P. Lettieri, L. Mazzei, R. Taylor, C. Chapman, Tar evolution in a two stage fluid bed–plasma gasification process for waste valorization, Fuel Process. Technol. 128 (2014) 146–157.
[148] F. Marias, R. Demarthon, A. Bloas, J. Robert-Arnouil, F. Nebbad, Design of a high temperature reactor fed by a plasma torch for tar conversion: comparison between CFD modelling and experimental results, Waste Biomass Valorization 6 (2015) 97–108.
[149] M. Materazzi, P. Lettieri, L. Mazzei, R. Taylor, C. Chapman, Reforming of tars and organic sulphur compounds in a plasma-assisted process for waste gasification, Fuel Process. Technol. 137 (2015) 259–268.
[150] A. Fourcault, F. Marias, U. Michon, Modelling of thermal removal of tars in a high temperature stage fed by a plasma torch, Biomass Bioenergy 34 (2010) 1363–1374.
[151] C. Du, H. Li, L. Zhang, J. Wang, D. Huang, M. Xiao, J. Cai, Y. Chen, H. Yan, Y. Xiong, Hydrogen production by steam-oxidative reforming of bio-ethanol assisted by Laval nozzle arc discharge, Int. J. Hydrogen Energy 37 (2012) 8318–8329.
[152] S. Nair, K. Yan, A. Pemen, E. Van Heesch, K. Ptasinski, A. Drinkenburg, Tar removal from biomass-derived fuel gas by pulsed corona discharges. A chemical kinetic study, Ind. Eng. Chem. Res. 43 (2004) 1649–1658.
[153] A. Jahanmiri, M. Rahimpour, M.M. Shirazi, N. Hooshmand, H. Taghvaei, Naphtha cracking through a pulsed DBD plasma reactor: effect of applied voltage, pulse repetition frequency and electrode material, Chem. Eng. J. 191 (2012) 416–425.
[154] F. Saleem, K. Zhang, A. Harvey, Temperature dependence of non-thermal plasma assisted hydrocracking of toluene to lower hydrocarbons in a dielectric barrier discharge reactor, Chem. Eng. J. (2018).
[155] F. Saleem, K. Zhang, A. Harvey, Role of CO_2 in the conversion of toluene as a tar surrogate in a nonthermal plasma dielectric barrier discharge reactor, Energy Fuels 32 (2018) 5164–5170.
[156] N. Hooshmand, M.R. Rahimpour, A. Jahanmiri, H. Taghvaei, M. Mohamadzadeh Shirazi, Hexadecane cracking in a hybrid catalytic pulsed dielectric barrier discharge plasma reactor, Ind. Eng. Chem. Res. 52 (2013) 4443–4449.
[157] H. Taghvaei, A. Jahanmiri, M.R. Rahimpour, M.M. Shirazi, N. Hooshmand, Hydrogen production through plasma cracking of hydrocarbons: effect of carrier gas and hydrocarbon type, Chem. Eng. J. 226 (2013) 384–392.
[158] M.R. Rahimpour, A. Jahanmiri, P. Rostami, H. Taghvaei, B.C. Gates, Upgrading of anisole in a catalytic pulsed dielectric barrier discharge plasma reactor, Energy Fuels 27 (2013) 7424–7431.
[159] H. Taghvaei, M. Kheirollahivash, M. Ghasemi, P. Rostami, M.R. Rahimpour, Noncatalytic upgrading of anisole in an atmospheric DBD plasma reactor: effect of carrier gas type, voltage, and frequency, Energy Fuels 28 (2014) 2535–2543.
[160] R. Cimerman, D. Račková, K. Hensel, Tars removal by non-thermal plasma and plasma catalysis, J. Phys. D Appl. Phys. 51 (2018) 274003.
[161] M. Rafiq, J. Hustad, Biosyngas production by autothermal reforming of waste cooking oil with propane using a plasma-assisted gliding arc reactor, Int. J. Hydrogen Energy 36 (2011) 8221–8233.
[162] X. Tu, J.C. Whitehead, Plasma dry reforming of methane in an atmospheric pressure AC gliding arc discharge: co-generation of syngas and carbon nanomaterials, Int. J. Hydrogen Energy 39 (2014) 9658–9669.
[163] T. Nunnally, A. Tsangaris, A. Rabinovich, G. Nirenberg, I. Chernets, A. Fridman, Gliding arc plasma oxidative steam reforming of a simulated syngas containing naphthalene and toluene, Int. J. Hydrogen Energy 39 (2014) 11976–11989.
[164] C.M. Du, J.H. Yan, B. Cheron, Decomposition of toluene in a gliding arc discharge plasma reactor, Plasma Sources Sci. Technol. 16 (2007) 791–797.
[165] D. Czylkowski, B. Hrycak, M. Jasiński, M. Dors, J. Mizeraczyk, Microwave plasma-based method of hydrogen production via combined steam reforming of methane, Energy 113 (2016) 653–661.
[166] L. Spencer, A. Gallimore, CO_2 dissociation in an atmospheric pressure plasma/catalyst system: a study of efficiency, Plasma Sources Sci. Technol. 22 (2012) 015019.
[167] P.G. Rutberg, A. Bratsev, V. Kuznetsov, V. Popov, A. Ufimtsev, On efficiency of plasma gasification of wood residues, Biomass Bioenergy 35 (2011) 495–504.
[168] G. Van Rooij, D. van den Bekerom, N. Den Harder, T. Minea, G. Berden, W. Bongers, R. Engeln, M. Graswinckel, E. Zoethout, M. van de Sanden, Taming microwave plasma to beat thermodynamics in CO_2 dissociation, Faraday Discuss. 183 (2015) 233–248.
[169] L. Jin, Y. Li, Y. Feng, H. Hu, A. Zhu, Integrated process of coal pyrolysis with CO_2 reforming of methane by spark discharge plasma, J. Anal. Appl. Pyrolysis 126 (2017) 194–200.
[170] Y.N. Chun, S.C. Kim, K. Yoshikawa, Removal characteristics of tar benzene using the externally oscillated plasma reformer, Chem. Eng. Process. Process. Intensif. 57 (2012) 65–74.
[171] X.S. Li, B. Zhu, C. Shi, Y. Xu, A.M. Zhu, Carbon dioxide reforming of methane in kilohertz spark-discharge plasma at atmospheric pressure, Aiche J. 57 (2011) 2854–2860.
[172] H. Zhang, F. Zhu, X. Li, K. Cen, C. Du, X. Tu, Rotating gliding arc assisted water splitting in atmospheric nitrogen, Plasma Chem. Plasma Process. 36 (2016) 813–834.
[173] H. Taghvaei, M. Kheirollahivash, M. Ghasemi, P. Rostami, B.C. Gates, M.R. Rahimpour, Upgrading of anisole in a dielectric barrier discharge plasma reactor, Energy Fuels 28 (2014) 4545–4553.
[174] F. Mushtaq, R. Mat, F.N. Ani, Fuel production from microwave assisted pyrolysis of coal with carbon surfaces, Energy Convers. Manage. 110 (2016) 142–153.
[175] C.M. Du, J.H. Yan, B. Cheron, Decomposition of toluene in a gliding arc discharge plasma reactor, Plasma Sources Sci. Technol. 16 (2007) 791.
[176] J. Gao, J. Zhu, A. Ehn, M. Aldén, Z. Li, In-situ non-intrusive diagnostics of toluene removal by a gliding arc discharge using planar laser-induced fluorescence, Plasma Chem. Plasma Process. 37 (2017) 433–450.
[177] H. Huang, D. Ye, D.Y. Leung, F. Feng, X. Guan, Byproducts and pathways of toluene destruction via plasma-catalysis, J. Mol. Catal. A Chem. 336 (2011) 87–93.
[178] H. Kohno, A.A. Berezin, J.-S. Chang, M. Tamura, T. Yamamoto, A. Shibuya, S. Honda, Destruction of volatile organic compounds used in a semiconductor industry by a capillary tube discharge reactor, IEEE Trans. Ind. Appl. 34 (1998) 953–966.
[179] J. Van Durme, J. Dewulf, W. Sysmans, C. Leys, H. Van Langenhove, Abatement and degradation pathways of toluene in indoor air by positive corona discharge, Chemosphere 68 (2007) 1821–1829.
[180] H.L. Chen, H.M. Lee, S.H. Chen, Y. Chao, M.B. Chang, Review of plasma catalysis

on hydrocarbon reforming for hydrogen production—interaction, integration, and prospects, Appl. Catal. B 85 (2008) 1–9.
[181] J. Van Durme, J. Dewulf, C. Leys, H. Van Langenhove, Combining non-thermal plasma with heterogeneous catalysis in waste gas treatment: a review, Appl. Catal. B 78 (2008) 324–333.
[182] C. Li, D. Hirabayashi, K. Suzuki, Steam reforming of biomass tar producing H_2-rich gases over Ni/MgO_x/CaO_{1-x} catalyst, Bioresour. Technol. 101 (2010) S97–S100.
[183] C. Wu, Q. Huang, M. Sui, Y. Yan, F. Wang, Hydrogen production via catalytic steam reforming of fast pyrolysis bio-oil in a two-stage fixed bed reactor system, Fuel Process. Technol. 89 (2008) 1306–1316.
[184] J.D. Holladay, J. Hu, D.L. King, Y. Wang, An overview of hydrogen production technologies, Catal. Today 139 (2009) 244–260.
[185] C.M. Kalamaras, A.M. Efstathiou, Hydrogen production technologies: current state and future developments, Conference Papers in Science (2013).
[186] S.A. Nair, Corona Plasma for Tar Removal, The dissertation of Eindhoven University of Technology, 2004.
[187] N. Wang, K. Shen, X. Yu, W. Qian, W. Chu, Preparation and characterization of a plasma treated NiMgSBA-15 catalyst for methane reforming with CO_2 to produce syngas, Catal. Sci. Technol. 3 (2013) 2278–2287.
[188] C. Zhang, D. Wang, M. Zhu, F. Yu, B. Dai, Plasma-enhanced copper dispersion and activity performance of Cu-Ni/ZrO_2 catalyst for dimethyl oxalate hydrogenation, Catal. Commun. 102 (2017) 31–34.
[189] B. Roldan Cuenya, Metal nanoparticle catalysts beginning to shape-up, Acc. Chem. Res. 46 (2012) 1682–1691.
[190] L.K. Ono, B. Roldan Cuenya, Formation and thermal stability of Au_2O_3 on gold nanoparticles: size and support effects, J. Phys. Chem. C 112 (2008) 4676–4686.
[191] Y. Zhou, T. Holme, J. Berry, T.R. Ohno, D. Ginley, R. O'Hayre, Dopant-induced electronic structure modification of HOPG surfaces: implications for high activity fuel cell catalysts, J. Phys. Chem. C 114 (2009) 506–515.
[192] H. Mistry, A.S. Varela, C.S. Bonifacio, I. Zegkinoglou, I. Sinev, Y.-W. Choi, K. Kisslinger, E.A. Stach, J.C. Yang, P. Strasser, Highly selective plasma-activated copper catalysts for carbon dioxide reduction to ethylene, Nat. Commun. 7 (2016) 12123.
[193] S. Zhang, X.-S. Li, B. Zhu, J.-L. Liu, X. Zhu, A.-M. Zhu, B.W.-L. Jang, Atmospheric-pressure O_2 plasma treatment of Au/TiO_2 catalysts for CO oxidation, Catal. Today 256 (2015) 142–147.
[194] R. Zhu, Y. Mao, L. Jiang, J. Chen, Performance of chlorobenzene removal in a nonthermal plasma catalysis reactor and evaluation of its byproducts, Chem. Eng. J. 279 (2015) 463–471.
[195] J. Aluha, N. Braidy, A. Dalai, N. Abatzoglou, Low-temperature Fischer-Tropsch synthesis using plasma-synthesized nanometric Co/C and Fe/C catalysts, Can. J. Chem. Eng. 94 (2016) 1504–1515.
[196] T. Fu, C. Huang, J. Lv, Z. Li, Fuel production through Fischer–Tropsch synthesis on carbon nanotubes supported Co catalyst prepared by plasma, Fuel 121 (2014) 225–231.
[197] W. Chu, J. Xu, J. Hong, T. Lin, A. Khodakov, Design of efficient Fischer Tropsch cobalt catalysts via plasma enhancement: Reducibility and performance, Catal. Today 256 (2015) 41–48.
[198] X. Tang, F. Gao, Y. Xiang, H. Yi, S. Zhao, Low temperature catalytic oxidation of nitric oxide over the Mn–CoO_x catalyst modified by nonthermal plasma, Catal. Commun. 64 (2015) 12–17.
[199] K. Li, X. Tang, H. Yi, P. Ning, Y. Xiang, J. Wang, C. Wang, X. Peng, Research on manganese oxide catalysts surface pretreated with non-thermal plasma for NO catalytic oxidation capacity enhancement, Appl. Surf. Sci. 264 (2013) 557–562.
[200] N. HafezKhiabani, S. Fathi, B. Shokri, S.I. Hosseini, A novel method for decoking of Pt–Sn/Al_2O_3 in the naphtha reforming process using RF and pin-to-plate DBD plasma systems, Appl. Catal. A Gen. 493 (2015) 8–16.
[201] N. Wang, W. Chu, T. Zhang, X.-S. Zhao, Manganese promoting effects on the Co–Ce–Zr–O_x nano catalysts for methane dry reforming with carbon dioxide to hydrogen and carbon monoxide, Chem. Eng. J. 170 (2011) 457–463.
[202] D. Liu, Y. Wang, D. Shi, X. Jia, X. Wang, A. Borgna, R. Lau, Y. Yang, Methane reforming with carbon dioxide over a Ni/ZiO_2–SiO_2 catalyst: influence of pre-treatment gas atmospheres, Int. J. Hydrogen Energy 37 (2012) 10135–10144.
[203] X. Yu, F. Zhang, N. Wang, S. Hao, W. Chu, Plasma-treated bimetallic Ni–Pt catalysts derived from hydrotalcites for the carbon dioxide reforming of methane, Catal. Letters 144 (2014) 293–300.
[204] F. Simescu-Lazar, V. Meille, S. Pallier, E. Chaînet, C. De Bellefon, Regeneration of deactivated catalysts coated on foam and monolith: Example of Pd/C for nitrobenzene hydrogenation, Appl. Catal. A Gen. 453 (2013) 28–33.
[205] C. Du, D. Huang, J. Mo, D. Ma, Q. Wang, Z. Mo, S. Ma, Renewable hydrogen from ethanol by a miniaturized nonthermal arc plasma-catalytic reforming system, Int. J. Hydrogen Energy 39 (2014) 9057–9069.
[206] H. Lee, D.-H. Lee, Y.-H. Song, W.C. Choi, Y.-K. Park, D.H. Kim, Synergistic effect of non-thermal plasma–catalysis hybrid system on methane complete oxidation over Pd-based catalysts, Chem. Eng. J. 259 (2015) 761–770.
[207] T.P. Huu, S. Gil, P. Da Costa, A. Giroir-Fendler, A. Khacef, Plasma-catalytic hybrid reactor: application to methane removal, Catal. Today 257 (2015) 86–92.
[208] B. Xu, J. Xie, H. Zhan, X. Yin, C. Wu, H. Liu, Removal of toluene as a biomass tar surrogate in a catalytic non-thermal plasma process, Energy Fuels 32 (2018) 10709–10719.
[209] M. Lu, R. Huang, J. Wu, M. Fu, L. Chen, D. Ye, On the performance and mechanisms of toluene removal by FeO_x/SBA-15-assisted non-thermal plasma at atmospheric pressure and room temperature, Catal. Today 242 (2015) 274–286.
[210] Y.-R. Zhang, K. Van Laer, E.C. Neyts, A. Bogaerts, Can plasma be formed in catalyst pores? A modeling investigation, Appl. Catal. B 185 (2016) 56–67.
[211] A. Pylinina, I. Mikhalenko, Activation of Cu-, Ag-, Au/ZrO_2 catalysts for dehydrogenation of alcohols by low-temperature oxygen and hydrogen plasma, Theor. Exp. Chem. 49 (2013) 65–69.
[212] E.C. Neyts, K. Ostrikov, M.K. Sunkara, A. Bogaerts, Plasma catalysis: synergistic effects at the nanoscale, Chem. Rev. 115 (2015) 13408–13446.
[213] R. Marques, S. Da Costa, P. Da Costa, Plasma-assisted catalytic oxidation of methane: on the influence of plasma energy deposition and feed composition, Appl. Catal. B 82 (2008) 50–57.
[214] G. Xiao, W. Xu, R. Wu, M. Ni, C. Du, X. Gao, Z. Luo, K. Cen, Non-thermal plasmas for VOCs abatement, Plasma Chem. Plasma Process. 34 (2014) 1033–1065.
[215] R. Huang, M. Lu, P. Wang, Y. Chen, J. Wu, M. Fu, L. Chen, D. Ye, Enhancement of the non-thermal plasma-catalytic system with different zeolites for toluene removal, RSC Adv. 5 (2015) 72113–72120.
[216] E. Neyts, A. Bogaerts, Understanding plasma catalysis through modelling and simulation—a review, J. Phys. D Appl. Phys. 47 (2014) 224010.
[217] N.A.S. Amin, Co-generation of synthesis gas and C_{2+} hydrocarbons from methane and carbon dioxide in a hybrid catalytic-plasma reactor: a review, Fuel 85 (2006) 577–592.
[218] X. Tu, J. Whitehead, Plasma-catalytic dry reforming of methane in an atmospheric dielectric barrier discharge: understanding the synergistic effect at low temperature, Appl. Catal. B 125 (2012) 439–448.
[219] D. Mei, X. Zhu, C. Wu, B. Ashford, P.T. Williams, X. Tu, Plasma-photocatalytic conversion of CO_2 at low temperatures: understanding the synergistic effect of plasma-catalysis, Appl. Catal. B 182 (2016) 525–532.
[220] F. Holzer, F. Kopinke, U. Roland, Influence of ferroelectric materials and catalysts on the performance of non-thermal plasma (NTP) for the removal of air pollutants, Plasma Chem. Plasma Process. 25 (2005) 595–611.
[221] K. Hensel, S. Katsura, A. Mizuno, DC microdischarges inside porous ceramics, Ieee Trans. Plasma Sci. 33 (2005) 574–575.
[222] K. Hensel, V. Martišovitš, Z. Machala, M. Janda, M. Leštinský, P. Tardiveau, A. Mizuno, Electrical and optical properties of AC microdischarges in porous ceramics, Plasma Process. Polym. 4 (2007) 682–693.
[223] M. Tsodikov, O. Ellert, S. Nikolaev, O. Arapova, G. Konstantinov, O. Bukhtenko, A.Y. Vasil'kov, The role of nanosized nickel particles in microwave-assisted dry reforming of lignin, Chem. Eng. J. 309 (2017) 628–637.
[224] R. Gulyaev, E. Slavinskaya, S. Novopashin, D. Smovzh, A. Zaikovskii, D.Y. Osadchii, O. Bulavchenko, S. Korenev, A. Boronin, Highly active $PdCeO_x$ composite catalysts for low-temperature CO oxidation, prepared by plasma-arc synthesis, Appl. Catal. B 147 (2014) 132–143.
[225] X. Zhu, S. Liu, Y. Cai, X. Gao, J. Zhou, C. Zheng, X. Tu, Post-plasma catalytic removal of methanol over Mn–Ce catalysts in an atmospheric dielectric barrier discharge, Appl. Catal. B 183 (2016) 124–132.
[226] S. Zhao, K. Li, S. Jiang, J. Li, Pd–Co based spinel oxides derived from Pd nanoparticles immobilized on layered double hydroxides for toluene combustion, Appl. Catal. B 181 (2016) 236–248.
[227] B. Wang, B. Chen, Y. Sun, H. Xiao, X. Xu, M. Fu, J. Wu, L. Chen, D. Ye, Effects of dielectric barrier discharge plasma on the catalytic activity of Pt/CeO_2 catalysts, Appl. Catal. B 238 (2018) 328–338.
[228] F. Rahmani, M. Haghighi, P. Estifaee, Synthesis and characterization of Pt/Al_2O_3–CeO_2nanocatalyst used for toluene abatement from waste gas streams at low temperature: conventional vs. plasma–ultrasound hybrid synthesis methods, Microporous Mesoporous Mater. 185 (2014) 213–223.
[229] T. Chang, Z. Shen, Y. Huang, J. Lu, D. Ren, J. Sun, J. Cao, H. Liu, Post-plasma-catalytic removal of toluene using MnO_2–Co_3O_4 catalysts and their synergistic mechanism, Chem. Eng. J. 348 (2018) 15–25.
[230] N. Jiang, L. Guo, C. Qiu, Y. Zhang, K. Shang, N. Lu, J. Li, Y. Wu, Reactive species distribution characteristics and toluene destruction in the three-electrode DBD reactor energized by different pulsed modes, Chem. Eng. J. 350 (2018) 12–19.
[231] X. Yao, J. Zhang, X. Liang, C. Long, Plasma-catalytic removal of toluene over the supported manganese oxides in DBD reactor: effect of the structure of zeolites support, Chemosphere 208 (2018) 922–930.
[232] J. Sun, Q. Wang, W. Wang, K. Wang, Study on the synergism of steam reforming and photocatalysis for the degradation of Toluene as a tar model compound under microwave-metal discharges, Energy 155 (2018) 815–823.